Journal of Physiology (1992), **456**, *pp.* 143–179
With 16 figures
Printed in Great Britain

ACTIVATION OF *N*-METHYL-D-ASPARTATE RECEPTORS BY L-GLUTAMATE IN CELLS DISSOCIATED FROM ADULT RAT HIPPOCAMPUS

BY A. J. GIBB AND D. COLQUHOUN

From the Department of Pharmacology, University College London, Gower Street, London WC1E 6BT

(*Received 10 December 1991*)

SUMMARY

1. Single channel recording techniques were used to study the ion channel openings resulting from activation of *N*-methyl-D-aspartate (NMDA) receptors by the agonist glutamate. Patches were from cells acutely dissociated from adult rat hippocampus (CA1). Channel activity was studied at low glutamate concentrations (20–100 nM) with 1 μM-glycine, in the absence of extracellular divalent cations.

2. Channel openings were to two main conductance levels corresponding to 50 pS and 40 pS openings in extracellular solution with 1 mM-Ca^{2+}. Around 80% of openings were to the large conductance level. The single channel conductances increased as extracellular Ca^{2+} was reduced.

3. Distributions of channel open times were described by three exponential components of 87 μs, 0·91 ms and 4·72 ms (relative areas of 51, 31 and 18%). Most long openings were to the large conductance level.

4. The channel closed time distribution was complex, requiring five exponential components to describe it adequately. Of these five components, at least three, with time constants of 68 μs, 0·72 ms and 7·6 ms (relative areas of 38, 12 and 17%) represent gaps within single activations of the receptor. The presence of a component with a mean of 7·6 ms is notable because gaps of this length have not previously been identified as being within single NMDA receptor channel activations.

5. Channel activations were identified as including gaps underlying at least the first three closed time components. Activations consisted of clusters of channel openings. Distributions of the length of these clusters had mean time constants of 88 μs, 3·4 ms and 32 ms (relative areas of 45, 25 and 30%). Long clusters contained short, intermediate and long duration openings as well as subconductance openings. The open probability within clusters averaged 0·62. Three components were evident in distributions of the number of openings per cluster. These had mean values of 1·22, 3·2 and 11 openings per cluster.

6. An inverse correlation was evident between the length of adjacent open and closed times. When open intervals were separated into groups based on the length of adjacent gaps, the time constants of the exponential components in these conditional open time distributions were independent of the length of the adjacent gap. This

supports the idea that the NMDA receptor channel gating has the properties of a discrete Markov process.

7. The long duration of NMDA receptor channel clusters suggests that they contribute to the slow time course of the NMDA receptor-mediated synaptic current.

INTRODUCTION

The most detailed studies of the single channel openings activated by neurotransmitters have used nicotinic acetylcholine receptors (AChR) from muscle endplate (Colquhoun & Sakmann, 1985), from the BC3H1 cell line (Sine & Steinbach, 1986, 1987), or electric organ receptors in fibroblasts (Sine, Claudio & Sigworth, 1990). In each case, interpretation of the single channel data has allowed estimation of the rates of the various reactions involved in receptor activation. For the endplate AChR, (Colquhoun & Sakmann, 1985), these rates are entirely consistent with what is known about synaptic transmission at the neuromuscular junction. This suggests that new insights into central excitatory synaptic transmission may be obtained by examining the single channel properties of glutamate receptors in central neurones.

In recent years a great deal of new information concerning the NMDA subtype of glutamate receptor has been obtained using patch clamp techniques in tissue cultured embryonic or young neurones (Nowak, Bregestovski, Ascher, Herbet & Prochiantz, 1984; Cull-Candy & Usowicz, 1987; Jahr & Stevens, 1987; Johnson & Ascher, 1987). In contrast, most studies concerning the role of the NMDA receptor in synaptic transmission (Herron, Lester, Coan & Collingridge, 1986; Collingridge, Herron & Lester, 1988; Thomson, Walker & Flynn, 1989; Hestrin, Nicoll, Perkel & Sah, 1990*a*; Mittman, Taylor & Copenhagen, 1990), long-term potentiation (see Collingridge & Singer, 1990, for review) or neural integration (Dale & Roberts, 1985) have used recordings from slices of adult brain or *in vivo* recordings. It is therefore desirable that the single channel properties of NMDA receptors should also be examined in adult neurones.

NMDA receptors mediate the slow component of excitatory postsynaptic potentials (EPSPs) in the central nervous system (Dale & Roberts, 1985; Forsythe & Westbrook, 1988; Collingridge *et al.* 1988; Thomson *et al.* 1989; Hestrin *et al.* 1990*a*). Voltage clamp experiments have demonstrated that the current (EPSC) that underlies the NMDA component has a slow rising phase (Hestrin *et al.* 1990*a*; Lester, Clements, Westbrook & Jahr, 1990; Stern, Edwards & Sakmann, 1992), and a slow decay time constant in the range of 50–150 ms (Forsythe & Westbrook, 1988; Collingridge *et al.* 1988; Hestrin *et al.* 1990*a*; Lester *et al.* 1990; Stern *et al.* 1992). More recent work has shown two exponential components in the decay of the NMDA receptor-mediated EPSC (Hestrin, Sah & Nicoll, 1990*b*; Lester *et al.* 1990; Keller, Konnerth & Yaari, 1991; Randall & Collingridge, 1991; Stern *et al.* 1992), and this may account for the wide range in decay time constants reported in earlier studies.

The experiments in this study were designed primarily to characterize the ion channel openings which result from a single activation of the NMDA receptor by glutamate. Channel openings produced by very low glutamate concentrations were studied (at which individual activations should be well separated). An activation is defined as the time from the start of the first opening after an agonist has bound to the receptor until the end of the opening which is followed by dissociation of all

agonist molecules from the receptor, so that the receptor returns to its resting, unoccupied state.

While providing evidence for some functional similarity between the NMDA receptor and the AChR, the results indicate that the NMDA receptor has some unique functional properties which may underlie the time course of the NMDA receptor-mediated component of the EPSC. A single NMDA receptor activation produces bursts of channel openings which are qualitatively similar to those observed for activation of AChRs (Colquhoun & Sakmann, 1985; Sine & Steinbach, 1986; Sine *et al.* 1990). However, about one-third of individual receptor activations produce not just one burst of openings, as for the AChR, but several bursts grouped together as a cluster. The closed periods between each burst within the activation are surprisingly long, being on average about 8 ms in duration with the possibility of additional closed periods in the order of 100 ms long also occurring. The duration of these clusters suggests that they contribute to the decay of the NMDA EPSC. Preliminary reports of some of this work, and related work have been published (Gibb, 1989, 1990; Gibb & Colquhoun, 1991).

METHODS

Solutions

A standard Krebs–Henseleit solution of composition (in mM): NaCl, 118; KCl, 2·5; $CaCl_2$, 2·5; $NaHCO_3$, 30; NaH_2PO_4, 1; $MgCl_2$, 1; glucose, 20; of pH 7·4 when bubbled with 95% O_2 and 5% CO_2, was used for preparation, enzyme treatment and maintenance of hippocampal slices. In some experiments the $MgCl_2$ concentration was raised to 10 mM and the $CaCl_2$ reduced to 0·2 mM during preparation with the aim of improving cell survival. For patch clamp recording, cells were bathed in a 'Mg^{2+}-free' Krebs' solution which was of the above composition, but with no added $MgCl_2$. The Krebs solution was bubbled with 95% O_2 and 5% CO_2 just before perfusion through the recording chamber. The free Mg^{2+} concentration in this solution was estimated by atomic absorbtion spectroscopy to be approximately 4 μM.

Single channel recordings were made using cell-attached or inside-out patch configurations (Hamill, Marty, Neher, Sakmann & Sigworth, 1981). The pipette solution was designed to have a low concentration of divalent cations (in particular, Mg^{2+}); it contained (in mM): NaCl, 118; EDTA, 10; $NaHCO_3$, 30; glucose, 20; to which was added 1 μM-glycine and an appropriate concentration of glutamate. This was bubbled with 95% O_2 and 5% CO_2 just before use, giving a pH of 7·4. In a few experiments an EGTA-buffered solution was used of composition: CsCl, 80; CsF, 60; HEPES, 12; EGTA, 11; equilibrated to pH 7·4 with NaOH, as an alternative to using EDTA as a divalent cation buffer.

Stock solutions of L-glutamate and glycine (Sigma or Fluka) were kept frozen, and thawed and diluted to the desired concentration each day before experimenting. All recordings were made at room temperature (20–24 °C).

Preparation of hippocampal slices

Standard procedures were used to prepare hippocampal slices from adult (200 g) male Sprague–Dawley rats. Rats were killed by cervical dislocation or chloroform overdose. This was followed rapidly by removal of the brain tissue into ice-cold ($\leqslant$ 4 °C) oxygenated Krebs solution. In some experiments animals that had been killed were perfused transcardially with ice-cold oxygenated Krebs solution before brain removal in order to obtain a more effective cooling of the brain tissue. The brain was hemisected and a flat surface cut across the dorsal side of one-half of the brain. This flat surface was glued to the tissue block of a Camden Vibroslice with cyanoacrylate glue, thus ensuring that the central part of the hippocampal formation was at right angles to the cutting blade. Slices were cut using Gillette stainless-steel or Camden vibroslice steel blades. The block of tissue was sliced at 500 μm thickness until clear transverse sections of hippocampus were evident. Three to five transverse slices of hippocampus and associated cortex were then cut. The CA1 region of each slice was dissected out with fine iridectomy scissors and each piece of CA1 region cut into two or three smaller pieces before being placed in a stirring chamber for enzyme treatment.

In a few later experiments thin (200 μm) slices (Edwards, Konnerth, Sakmann & Takahashi, 1989) were cut, and patches made from cells in these slices without prior enzyme treatment or dissociation.

Cell dissociation

Cells were dissociated using methods similar to those of and Kay & Wong (1986). Pieces of hippocampal CA1 region were incubated at room temperature (20–24 °C) in 10 ml of standard Krebs solution containing 1 mg/ml papain plus 1 mM-cysteine (both Sigma) or 1 mg/ml trypsin (Sigma Type XI). In addition the enzyme solution contained 0·1 mg/ml elastase and 0·1 mg/ml DNase (both Sigma). The tissue pieces were stirred in this solution for 90 min, at a rate just sufficient to prevent them from settling to the bottom of the beaker. This was achieved using a small magnetic stirrer bar mounted on a central glass pillar 1 cm above the base of the 2 cm diameter by 3 cm deep stirring chamber. During enzyme treatment a 95% O_2, 5% CO_2 mixture was continuously blown onto the surface of the enzyme solution. After trypsin treatment, tissue pieces were stirred for a further 15 min in Krebs solution containing 1 mg/ml bovine trypsin inhibitor before being placed on a net in Krebs solution in a standard brain slice holding-chamber which was continuously bubbled with 95% O_2 and 5% CO_2. Tissue pieces could be kept in this way for up to 8 h.

Cells were mechanically dissociated by gently triturating two or three tissue pieces, suspended in 1 ml of Krebs solution, with a fire-polished Pasteur pipette of tip diameter 2–3 mm until the tissue pieces were broken into small pieces. A Pasteur pipette fire-polished to a 1 mm tip opening was then used to complete the dissociation. The resulting suspension of cells and debris was decanted into a 1 cm high, 1 cm diameter plastic ring sealed with silicone grease onto a glass coverslip. Just prior to use, glass coverslips were dipped in a 1% solution of Alcian Blue dye and then washed in Krebs solution before being attached to the base of the recording chamber with a ring of Vaseline grease. The plastic ring around the coverslip ensured that cells settled onto the coverslip where the Alcian Blue dye aids firm attachment of the cells. The ring was removed after 5 min settling time and the bath was constantly perfused with pre-oxygenated Mg^{2+}-free Krebs solution at 2–3 ml/min for a further 5–10 min before experimental recording began.

Data recording

Patch clamp recordings were made using a List EPC7 or Axopatch 1B patch clamp amplifier. Patch electrodes were pulled from thick-walled borosilicate glass (Clark Electromedical GC150F-7.5), coated to within 100 μm of the tip with Sylgard resin (Dow Corning 184) and fire-polished on a Narashige (MF-83) microforge to a final tip resistance of 8–12 MΩ. The pipette resistance was adjusted according to the glutamate concentration in use as higher resistance pipettes were necessary to avoid multiple openings occurring in the data record at higher glutamate concentrations.

Cells were viewed under phase contrast optics on the stage of an upright microscope using a 40×, 0·75 numerical aperture, water-immersion objective with 1·6 mm working distance at a total magnification of 400×. Healthy cells were identified by their phase-bright appearance, apparently smooth surface and the presence of short stumps of broken-off dendrites.

Inside-out patches were usually voltage clamped at −60 mV although recordings were made at potentials between −100 and +100 mV. For cell-attached patches the pipette potential was usually clamped at 0 mV: cell resting potentials were estimated to be in the range of −40 to −75 mV. In a few cases outside-out patches were used to check that channels activated by bath perfusion of glutamate had essentially the same characteristics as those measured in inside-out or cell-attached patches (see also Gibb & Colquhoun, 1991). Outside-out patches were made using the same pipette solution as used for cell-attached and inside-out patches (see Solutions) but without any added glycine or glutamate. Single channel currents were stored on FM tape (Racal Store 4, DC-5 kHz) after filtering at 10 kHz (−3 dB, 8-pole Bessel response).

Data analysis

Single channel data records were replayed from FM tape, amplified and filtered at from 1–4 kHz (−3 dB, 8-pole Bessel), and continuously sampled at 10–40 kHz onto a PDP 11/73 computer hard disc using a CED 502 interface (Cambridge Electronic Design). The duration of open and closed periods in the data record was measured using the method of time course fitting (Colquhoun & Sigworth, 1983) after first estimating the amplitude of each channel opening using manually

controlled cursors placed on the data display. An idealized record of the durations and amplitudes of every detectable event in the data record was obtained by imposing a fixed resolution for open times and closed times. This was typically 60–80 μs for open times and 40–60 μs for closed times. The time course fitting method allows measurement of the duration of contiguous open states so that subconductance levels could be included in the analysis. An amplitude change of greater than 10% of the open channel current was regarded as significant during subsequent analysis. It is not possible to estimate accurately the amplitude of very brief channel openings, so amplitude histograms contained only values measured from openings of duration at least $2t_r$, where t_r is the filter rise-time of the recording system (e.g. Colquhoun & Sigworth, 1983). For openings shorter than $2t_r$ their duration was measured after assuming their amplitude to be equal to the mean amplitude of the clearly resolved openings in the data record. Short attenuated closings were assumed to be complete unless there was clear evidence that the transition was to a subconductance level. The essential ambiguity involved in distinguishing between short closings and short dwell times at a subconductance level has been described elsewhere (Colquhoun & Sakmann, 1984; Howe, Cull-Candy & Colquhoun, 1991). In this study direct transitions between different open levels were identified when no shutting longer than the shut time resolution could be detected between two open periods, both open periods being at least $2t_r$ in duration.

Distributions conditional on event amplitude were constructed using a critical amplitude value, A_{crit}, which was calculated from the components fitted to the amplitude distribution so as to minimize the percentage of overlap between different components in the amplitude distribution as described by Howe *et al.* (1991).

Histograms of the distribution of open times and shut times, and properties of bursts of openings and clusters of bursts were constructed for display and evaluation of the data. In most cases the distribution of log (duration) is used for display purposes (Blatz & Magleby, 1986; Sigworth & Sine, 1987), with a square root transformation of the ordinate (Sigworth & Sine, 1987).

Distributions were fitted with the sum of several exponential, Gaussian or geometric components where appropriate. The individual observations of open times, shut times, etc. were fitted using the method of maximum likelihood (Colquhoun & Sigworth, 1983; Colquhoun & Sakmann, 1985).

Definition of bursts and clusters of bursts

Bursts of openings were defined as openings separated by closed times shorter than a critical length t_c. This was calculated so as to make the percentage of long closed times that were misclassified as within bursts equal to the percentage of short closed times that were misclassified as being between bursts (Colquhoun & Sakmann, 1985). For each patch t_c was calculated from the best-fit parameters of the closed time distribution treating components two and three as being 'within bursts' closed times respectively. To identify clusters of bursts, t_c was calculated in an exactly analogus way using components 3 and 4 of the closed time distribution. In addition, the length of 'super-clusters' in the data was examined by defining a critical gap length using components 4 and 5 in the shut time distribution (Gibb & Colquhoun, 1991).

Tests for correlations in the data

The runs test and autocorrelation coefficients (Colquhoun & Sakmann, 1985; Colquhoun & Hawkes, 1987) were calculated to test for correlations in the data. In addition, the mean and distribution of the lengths of open times adjacent to closed times within particular ranges were calculated (Blatz & Magleby, 1989; McManus & Magleby, 1989). This analysis of adjacent intervals provides an alternative to the calculation of the correlation between the length of an open time and its adjacent shut time and allows the visual display of results as conditional open time distributions. Distributions were constructed using both the preceding and the following opening adjacent to a particular closed time. Thus each open time was actually used twice. This procedure is justified provided the channel obeys the law of microscopic reversibility (Colquhoun & Hawkes, 1982; Läuger, 1983; Blatz & Magleby, 1989; but see also Cull-Candy & Usowicz, 1987).

In order to obtain sufficient numbers of intervals in each conditional open time distribution, it was necessary to define appropriate ranges of closed times. These closed time ranges were chosen for each patch by calculating critical closed times which minimize the percentage of overlap between pairs of components in the closed time distribution using the same procedure as used to determine the critical gap length, t_c, used to define bursts of openings. Thus the first closed time range includes closed times between the closed time resolution and a t_c value calculated using the first two components of the closed time distribution. The second closed time range was from this t_c value to

a critical closed time calculated using components 2 and 3 of the shut time distribution, and so on. In this way the five components present in the closed time distributions generated five closed time ranges.

RESULTS

Multiple conductance states of glutamate-activated channels

Single channel recordings from tissue-cultured embryonic cerebellar or hippocampal cells (Cull-Candy & Usowicz, 1987, 1989; Jahr & Stevens, 1987) have demonstrated that glutamate activates multiple conductance level channels ranging in conductance from 5 to 50 pS (in 1 or 2 mM-external Ca^{2+} concentration). Subsequent studies in cultured cerebellar granule cells have found similar multiple conductances (Howe, Colquhoun & Cull-Candy, 1988; Howe *et al.* 1991). In cells dissociated from adult rat hippocampus we find also that glutamate activates multiple conductance channels.

Conductances at low and high glutamate concentrations

Figure 1*A* shows representative records of channel openings recorded from an outside-out patch (the pipette solution contained Na^+ as the main cation and EDTA to buffer divalent cations as described in the Methods) in response to bath perfusion with 1 μM-glutamate in normal Krebs solution (containing 2·5 mM-Ca^{2+}, but with Mg^{2+} omitted) with no added glycine. In the absence of extracellular glutamate, channel openings were rare. In the presence of glutamate, channel openings to several different conductance levels were observed. Figure 1*B* shows the distribution of channel amplitudes measured in this patch, at -100 mV membrane potential. The distribution is fitted with the sum of five Gaussian components with the standard deviation constrained to be the same for each component. These five components had fitted parameters of (mean, (relative area)) 1·16 pA (7%), 1·82 pA (21%), 2·53 pA (27%), 3·33 pA (12%) and 4·25 pA (0·34%), the common standard deviation being 0·24 pA. This distribution is constructed from 287 amplitude measurements, of which fourteen were connected by apparently direct transitions to other open levels. Of these fourteen direct transitions, eleven occurred between amplitudes in the largest three amplitude levels and no direct transitions were detected between the smaller two and the larger three levels.

Most inside-out patch recordings were made with normal calcium in the bath since cell survival was poor in the 'zero divalents' solution. The presence of millimolar Ca^{2+} on the inner surface of the patch membrane did not seem to influence the channel behaviour since results obtained with cell-attached or inside-out patch recordings were very similar (see shut times and open times below) and in a few patches when the bath solution was changed to 'zero divalents' solution there was no change in the channel kinetics or conductance. Use of low glutamate concentrations with added glycine (rather than using 1 μM-glutamate and no added glycine) results in more selective activation of NMDA receptors and minimizes non-NMDA receptor activation.

Figure 1*C* shows examples of channel openings recorded from an inside-out patch at a membrane potential of -100 mV where the pipette was filled with EDTA-buffered 'zero divalents' solution containing 30 nM-glutamate and 1 μM-glycine. At this low glutamate concentration most openings were to the two highest levels. The

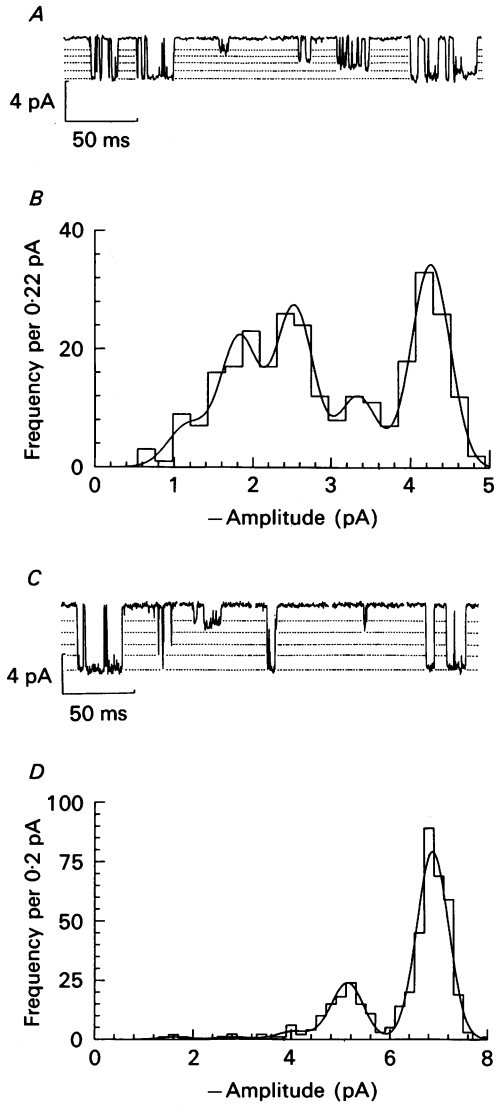

Fig. 1. *A*, single channel currents activated by 1 μM-glutamate in normal Krebs solutions with no added Mg^{2+} or glycine in an outside-out patch held at −100 mV. Examples of channel openings (downwards) to each of five different conductance levels identified. The dashed lines show where the current levels identified from the fit to the amplitude distribution shown in *B* would fall. The currents were low-pass filtered at 2 kHz (−3 dB). *B*, distribution of 287 channel amplitudes of openings longer than 0·332 ms measured from the same patch as shown in *A*. The distribution is shown fitted with the sum of five Gaussian components where the standard deviation is constrained to be the same for each component. These had fitted parameters of (mean ± S.D. (relative area)): 1·16 ± 0·24 pA (7%), 1·82 pA (21%), 2·53 pA (27%), 3·33 pA (12%) and 4·25 pA (34%). *C*, single-channel currents activated by 30 nM-glutamate plus 1 μM-glycine in EDTA-buffered 'zero-divalents' solution recorded from an inside-out patch held at −100 mV. Examples of channel openings (downwards) to each of five different conductance levels identified. The dashed lines show where the current levels identified from the fit to the amplitude distribution shown in *D* would fall. The currents were low-pass filtered at 2 kHz (−3 dB). *D*, distribution of 443 channel amplitudes of openings longer than 0·166 ms measured

distribution of amplitudes measured in this recording is shown in Fig. 1*D* fitted with five Gaussian components. The fitted parameters were (mean, (relative area)) 1·62 pA (0·7%), 3·02 pA (1·0%), 4·3 pA (3·5%), 5·18 pA (18%) and 6·86 pA (76%), with a common standard deviation of 0·32 pA. Of the 443 openings used to construct this distribution, 126 were connected by apparently direct transitions to another open level. One hundred of these direct transitions were between the largest two amplitude levels, eighteen were between the largest and the third largest level and the eight remaining direct transitions were between the largest two and smallest three conductance levels. Since very few apparently direct transitions are evident between the small conductance and large conductance levels, it is doubtful if the observed small conductance openings represent NMDA receptor channel openings (a similar conclusion was drawn by Howe *et al.* 1991). They could, for example, be occasional openings of non-NMDA receptor channels, which may still occur even at these very low glutamate concentrations. Whatever the origin of the small conductance openings, it is clear that in these dissociated hippocampal cells NMDA receptor activation mainly produces the two largest conductance levels.

Figure 2*A* shows single channel current–voltage relationships for the conductance levels observed in the outside-out patch illustrated in Fig. 1*A* and *B* where the extracellular solution was Mg^{2+}-free normal Krebs solution (2·5 mM-Ca^{2+}) containing 1 μM-glutamate and no added glycine. The slopes correspond to conductances of 44, 34, 26, 19 and 13 pS with a reversal potential of −6·5 mV. Figure 2*B* shows the current–voltage relationship for the principle subconductance and main conductance levels identified in the patch illustrated in Fig. 1*C* and *D*. The slope conductances of these are 57 and 73 pS respectively, with a predicted reversal potential of −7 mV in both cases.

Effect of Ca^{2+} on conductance

Detailed measurements of channel amplitudes were made on twenty-six patches, of which sixteen were inside-out and ten were cell-attached, all with EDTA-buffered extracellular solution. Outside-out patch recordings were found to be unstable in EDTA-buffered solution. The conductance levels were similar in both cell-attached and inside-out patch configurations. For all twenty-six patches the largest component of the amplitude distribution represented 77 ± 4% of the total area of the amplitude distribution. In the twelve inside-out patches, the main single channel conductance averaged 66 ± 1·4 pS, and the second conductance level averaged 50 ± 3 pS (assuming a 0 mV reversal potential), in the absence of extracellular Ca^{2+}. With 1 mM-external Ca^{2+} the conductances were lower, the mean results from seven outside-out patches (where channels were activated with 50 nM-glutamate plus 1 μM-glycine) being 51 ± 1·5 and 37 ± 1·5 pS. These are very similar to the main conductances of NMDA channels observed by Howe *et al.* (1991) and by Traynelis & Cull-Candy (1991). As illustrated above (Fig. 2*A*), NMDA channel conductances are lower still in 2·5 mM-external Ca^{2+}, the mean values for three patches (two inside-out

from the same patch as illustrated in *C*. The distribution is shown fitted with the sum of five Gaussian components where the standard deviation is constrained to be the same for each component. These had fitted parameters of (mean ± S.D. (relative area)): 1·62 ± 0·32 pA (0·7%), 3·02 pA (1%), 4·3 pA (3·5%), 5·18 pA (18%) and 6·86 pA (76%).

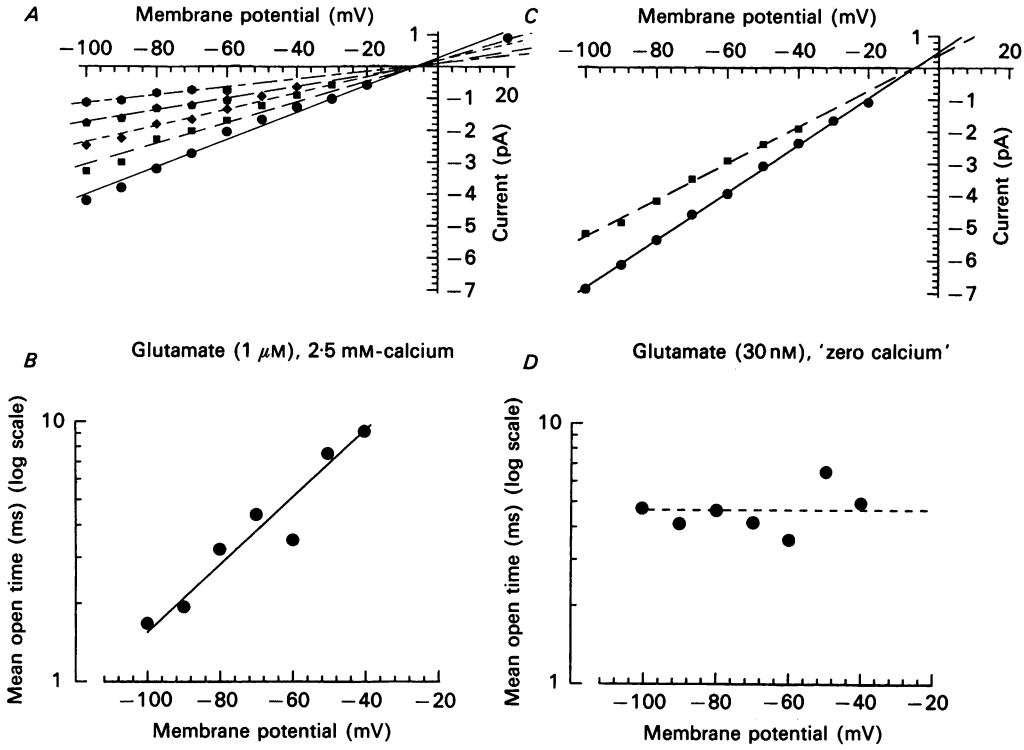

Fig. 2. *A*, relationship between single channel current amplitudes and patch potential for the outside-out patch illustrated in Fig. 1*A* and *B*. Channels activated by 1 μM-glutamate in normal Krebs solution (2·5 mM-Ca^{2+} with no added Mg^{2+} or glycine). The different symbols show the mean single channel current estimated from multiple Gaussian fits to the amplitude distribution obtained at each membrane potential. The continuous line shows a least-squares fit to the largest amplitude class which gave a conductance of 44 pS and reversal potential of −6·5 mV. The dashed lines show least squares fits to the lower amplitude classes where the reversal potential was constrained to be −6·5 mV in each case. These lines give conductance values of 34, 26, 19 and 13 pS. *B*, semilogarithmic plot of the mean apparent open time of openings underlying the largest Gaussian component identified in fits to the amplitude distributions used to generate the current–voltage relation shown in *A*. The continuous line shows the linear least-squares fit to the results which predicts an e-fold increase in open time per 34 mV depolarization. *C*, relationship between single channel current amplitudes and patch potential for the inside-out patch illustrated in Fig. 1*C* and *D*. Channels activated by 30 nM-glutamate plus 1 μM-glycine in EDTA-buffered 'zero-divalents' solution. The filled circles and filled squares show respectively the mean single channel current estimated from the two main components of multiple Gaussian fits to the amplitude distributions obtained at each membrane potential. The continuous and dashed lines are linear least-squares fits to the data which predict slope conductances of 57 and 73 pS respectively and a reversal potential of −7 mV in both cases. *D*, semilogarithmic plot of the mean apparent open time of openings underlying the largest Gaussian component identified in fits to the amplitude distributions used to generate the current–voltage relation shown in *B*. The dashed line shows where the mean of the measured mean open times would lie.

and one outside-out) being $42 \pm 0{\cdot}7$ and $33 \pm 0{\cdot}3$ pS. Thus the external concentration of Ca^{2+} has a strong effect on the single channel conductance (see also Ascher & Novak, 1988), the conductance being 50–60% greater in zero Ca^{2+} than in 2·5 mM-Ca^{2+} (similar for the two main conductance levels). When using extracellular solutions containing 150 mM-Na^+, the channel commonly referred to as '50 pS' is close to this conductance only at about 1 mM-Ca^{2+}. A similar effect has been observed in the case of nicotinic receptors of both muscle (Colquhoun & Sakmann, 1985) and neuronal type (Mathie, Cull-Candy & Colquhoun, 1987; Mathie, Colquhoun & Cull-Cundy, 1991).

Direct transitions between open states

In four patches only one conductance level was evident, whereas in fifteen other patches two conductance levels were detected, and in seven patches a third conductance level was evident. The frequency of direct transitions between subconductance levels and the largest conductance level was assessed in seventeen patches (five cell-attached and twelve inside-out). Although direct transitions between conductance levels were rare, they were consistently detected. On average $7{\cdot}1 \pm 1{\cdot}4$% of large conductance openings were connected by an apparently direct transition to another open level: $2{\cdot}5 \pm 0{\cdot}5$% of openings longer than $2t_r$ were connected by a direct transition *from* the large conductance level and $2{\cdot}2 \pm 0{\cdot}5$% of openings longer than $2t_r$ were connected by a direct transition *to* the large conductance level. This suggests that the channel obeys microscopic reversibility. The frequency of direct transitions to and from the large conductance level and the relative amplitude of the conductance levels is similar to that observed with NMDA receptor channels in cerebellar granule cells (Howe *et al.* 1991). The conductance levels themselves are also similar to the conductance levels observed in large cerebellar neurones in culture (Cull-Candy & Usowicz, 1987, 1989), but their quantitative behaviour is different. In particular, sublevel transitions in the large cerebellar neurones displayed temporal asymmetry suggesting that the channel did not obey microscopic reversibility and the frequency of direct transitions between 38 and 18 pS levels was much greater than observed here.

Effect of contaminant magnesium

Preliminary experiments demonstrated that the apparent open times were clearly dependent on membrane potential when using normal extracellular solution. This is illustrated in Fig. 2*C* where the open times became shorter with patch hyperpolarization with a voltage dependence, over the range -40 to -100 mV, which corresponded to e-fold shortening for 34 mV hyperpolarization (see also Howe *et al.* 1991). Analysis of the extracellular solution indicated that it contained approximately 4 μM-magnesium contamination; this suggests the possibility that the voltage dependence of the open times was due to magnesium block of the NMDA channel (Nowak *et al.* 1984). All subsequent experiments were therefore performed with an EDTA-buffered extracellular solution (see Methods), in which the concentration of free divalent cations should be less than 100 nM. Under these conditions the length of apparent open times appeared to be independent of membrane potential (Fig. 2*D*). Interestingly, the closed times showed no obvious voltage dependence in either normal or EDTA-buffered solutions.

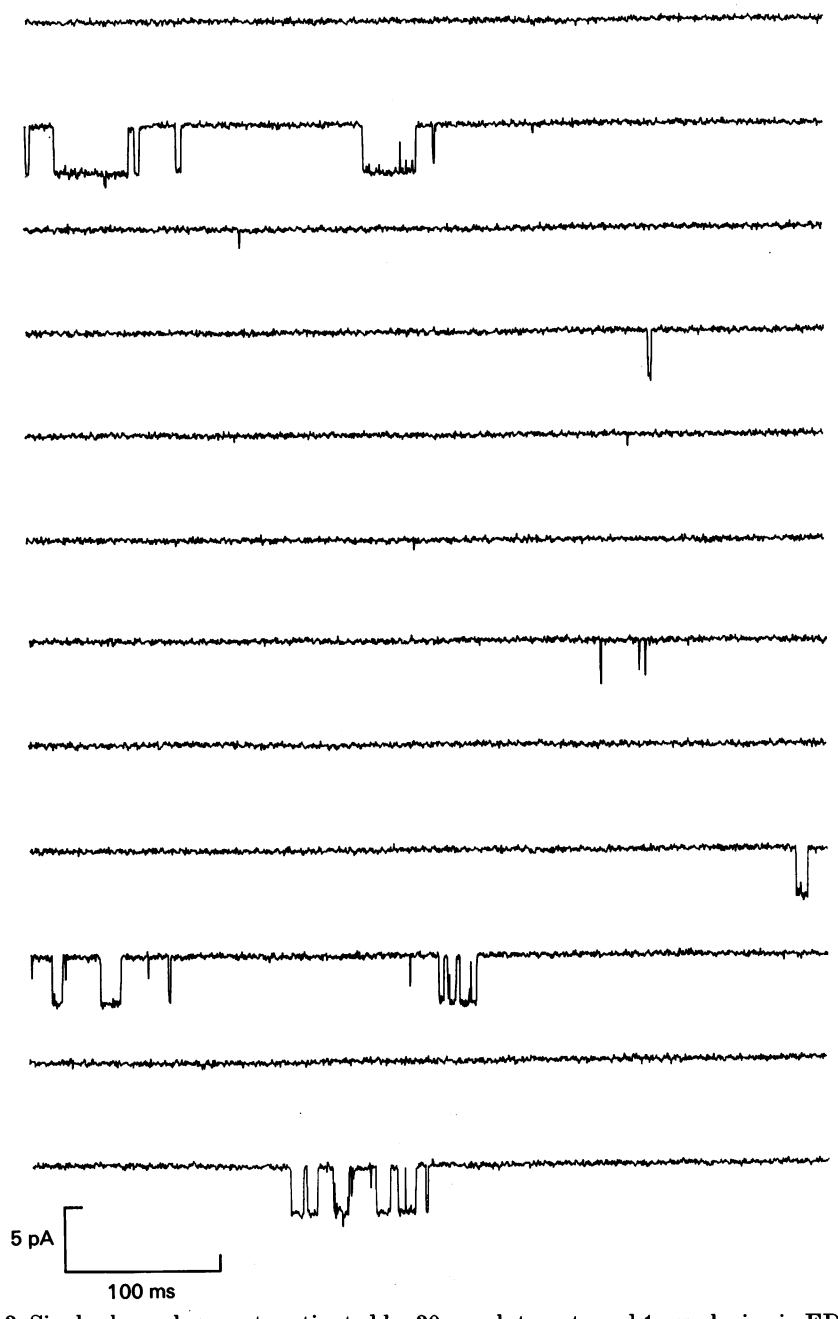

Fig. 3. Single channel currents activated by 30 nM-glutamate and 1 μM-glycine in EDTA-buffered 'zero divalents' solution. From an inside-out patch clamped at −60 mV. Channel openings (downwards) occur in bursts and clusters of bursts. Successive horizontal traces show twelve contiguous 500 ms sweeps to demonstrate the pattern of channel activation seen at these low glutamate concentrations. Currents were low-pass filtered at 2 kHz (−3 dB).

Channel activation properties at low glutamate concentrations

NMDA receptor channels were studied using low glutamate concentrations (20–100 nM) and 1 μM-glycine in order to activate NMDA receptors selectively. EDTA-buffered extracellular solution was used to avoid block of the NMDA channels by contaminant magnesium. Low glutamate concentrations were necessary to try to ensure that individual activations of the ion channel were well separated, and therefore clearly distinguishable from one another. The durations of shut times between individual activations will depend on the number of channels in the patch (which is not known), and also on the occurrence of desensitization; such shut times are not, therefore, easily interpretable. On the other hand open and shut times *within* a single activation are more easily interpreted because the entire activation will, almost certainly, originate from one individual receptor channel.

Figure 3 shows part of a 130 s recording from an inside-out patch with the extracellular surface of the patch bathed in EDTA-buffered solution containing 30 nM-glutamate and 1 μM-glycine. The trace shows a continuous recording of 6 s of data with the patch potential clamped at −60 mV. Several qualitative features are evident. There are some long closed periods, as would be expected at such a low agonist concentration. Openings sometimes occur singly (some of these are only partly resolved at the recording bandwidth used), but more usually the openings occur in groups, though these groups contain some surprisingly long gaps. Even at this very low agonist concentration, it is difficult to be sure by visual inspection of the record where each individual receptor activation begins and ends. However, consideration of the shut time distribution allows some conclusions to be drawn.

Shut time distributions

Distributions of channel shut times, such as that shown in Fig. 4*A*, were generally fitted with five exponential components. For twenty-six patches containing channels activated by glutamate concentrations between 20 and 100 nM, the mean time constants (and relative areas) of the shut time distribution components were $\tau_1 = 68 \pm 7$ μs (38 ± 3%), $\tau_2 = 0{\cdot}72 \pm 0{\cdot}12$ ms ($13 \pm 1{\cdot}5$%), $\tau_3 = 7{\cdot}56 \pm 0{\cdot}8$ ms (17 ± 2%), $\tau_4 = 137 \pm 26$ ms (22 ± 4%) and $\tau_5 = 922 \pm 195$ ms (18 ± 3%). The distribution means averaged 192 ± 48 ms. The shut time distribution is thus much more complex than that for the endplate nicotinic acetylcholine receptor which, under comparable conditions, shows only a very short (20 μs), and a very long component (e.g. 700 ms) (with a small intermediate component of around 0·5 ms) (Colquhoun & Sakmann, 1985).

The time constants of the two longest components varied between patches, and, when tested on outside-out patches (see Gibb & Colquhoun, 1991) at least the longest component depended on the glutamate concentration. On the other hand, the three shorter time constants (Fig. 4*B*) were fairly consistent between patches and did not vary with agonist concentration (Gibb & Colquhoun, 1991). In four patches out of a total of twenty-six patches analysed, the third shut time component, was not detected. However, in all other patches a component with a time constant of around 8 ms was evident. It is likely that these gaps occur within receptor activations (see Discussion below, and Gibb & Colquhoun, 1991).

There was no clear evidence that the time constants or relative areas of the fastest three shut time components were dependent on glutamate concentration (though the effects of different glutamate concentrations were measured on different inside-out patches, so variation between patches could have obscured any concentration

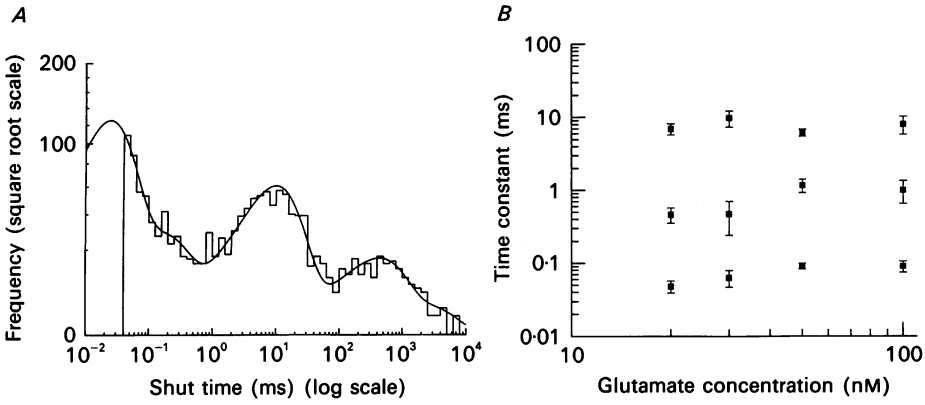

Fig. 4. *A*, distribution of all closed times greater than 40 μs in duration (n = 1377 gaps) recorded from the same patch as illustrated in Fig. 3. The histogram shows the distribution of log time *versus* the square root of bin frequency on the abscissa. The transformation converts the normal exponential distribution into a peaked function: each peak corresponds to the time constant of each exponential component. The distribution is shown fitted with the sum of five exponential components with time constants (and relative areas) of: 23 μs (53%), 0·15 ms (12%), 9·89 ms (27%), 411 ms (7·1%), 2·1 s (1%). The fit predicts the presence of 2579 gaps. The resolution was 50 μs for open times and 40 μs for closed times. The record was filtered at 3 kHz (−3 dB). *B*, double logarithmic plot of the mean time constants of the first three shut time components as a function of glutamate concentration. Time constants are shown as the means ± S.E.M. with n = 5–8.

dependence). In a related study using outside-out patches, where the concentration dependence of the shut time components was assessed, only the slowest of the shut time components was clearly dependent on glutamate concentration (Gibb & Colquhoun, 1991).

We were interested in seeing whether the patch configuration had any influence on the NMDA channel properties. For ten cell-attached patches the shut time distribution parameters averaged 80 ± 10 μs (29 ± 5%), 0·96 ± 0·21 ms (12 ± 3%), 9·07 ± 1·3 ms (10 ± 3%), 127 ± 24 ms (30 ± 8%) and 853 ± 209 ms (19 ± 5%). For sixteen inside-out patches the shut time distribution parameters averaged 62 ± 9 μs (41 ± 3%), 0·55 ± 0·12 ms (12 ± 2%), 6·7 ± 0·97 ms (17 ± 3%), 145 ± 41 ms (14 ± 3%) and 969 ± 299 ms (15 ± 5%).

Distributions of apparent open times

The distribution of channel closed times indicates that a considerable number of short closed times in the data record are missed due to the limited time resolution of the recording. Many of the measured open times in the data record must therefore contain unresolved gaps, resulting in an over-estimation of the duration of channel openings. However, the distribution of these apparent open times may still contain

much useful information relevant to the channel activation mechanism, especially where there is more than one exponential component in the distribution (Blatz & Magleby, 1989; McManus & Magleby, 1989; Hawkes, Jalali & Colquhoun, 1992).

The distribution of apparent open times contained three exponential components (Fig. 5). For the twenty-six patches analysed in this study the mean time constants

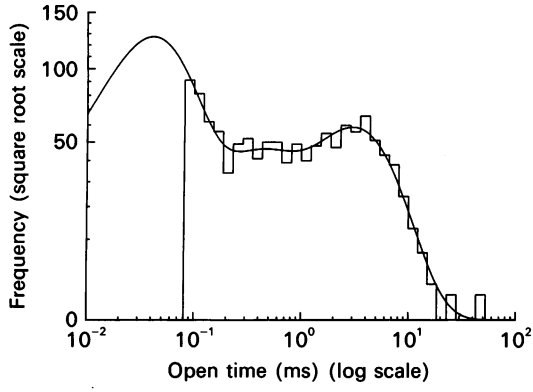

Fig. 5. Distribution of the length of 1206 apparent open times between 80 μs and 20 ms long. The distribution is fitted with the sum of three exponential components with parameters of 38 μs (57%), 0·27 ms (15%) and 2·93 ms (29%). The fit predicts that there were 2641 openings in the data record.

(and relative areas) of these components were 87 ± 9 μs (51 ± 4%), $0{\cdot}91 \pm 0{\cdot}16$ ms (31 ± 3%) and $4{\cdot}72 \pm 0{\cdot}6$ ms (18 ± 3%). These distributions had a mean of $1{\cdot}22 \pm 0{\cdot}23$ ms.

There was no evidence to suggest that the channel open times were different between cell-attached and inside-out patches. For the ten cell-attached patches the open time distribution parameters averaged 86 ± 9 μs (57 ± 4%), $0{\cdot}67 \pm 0{\cdot}14$ ms (32 ± 3%) and $4{\cdot}11 \pm 0{\cdot}44$ ms (11 ± 4%). For the sixteen inside-out patches these were 88 ± 15 μs (48 ± 6%), $1{\cdot}03 \pm 0{\cdot}24$ ms (30 ± 4%) and $5{\cdot}09 \pm 0{\cdot}44$ ms (23 ± 4%). This contrasts with the results of Covarrubias & Steinbach (1990) who found that the mean open time of muscle nicotinic AChRs is reduced following patch excision (see also Trautmann & Sigelbaum, 1983).

Missed events

The distributions of the apparent open and shut times just described suggest that there is likely to be a substantial number of both shuttings and openings that are too short to be detected. For example, with a typical resolution of 50 μs for shut times, about 48% of the shuttings in the 68 μs component (i.e. about 18% of all shut periods) would be too short to be detected. Similarly with a typical resolution of 70 μs for open times, about 45% of the openings in the 87 μs component (i.e. about 24% of all open times) would be too short to be detected. Unfortunately the complex burst structure of the channel activity, and the lack, so far, of any plausible mechanism to describe it, preclude any realistic correction of the observed distributions for these missed events (Hawkes *et al.* 1992).

Distributions of open times conditional on the amplitude of the openings

For each patch where more than one Gaussian component was detected in the amplitude distribution, distributions were constructed of the durations of 'full openings' (those to the main conductance level) and 'sublevel openings' (i.e. mainly

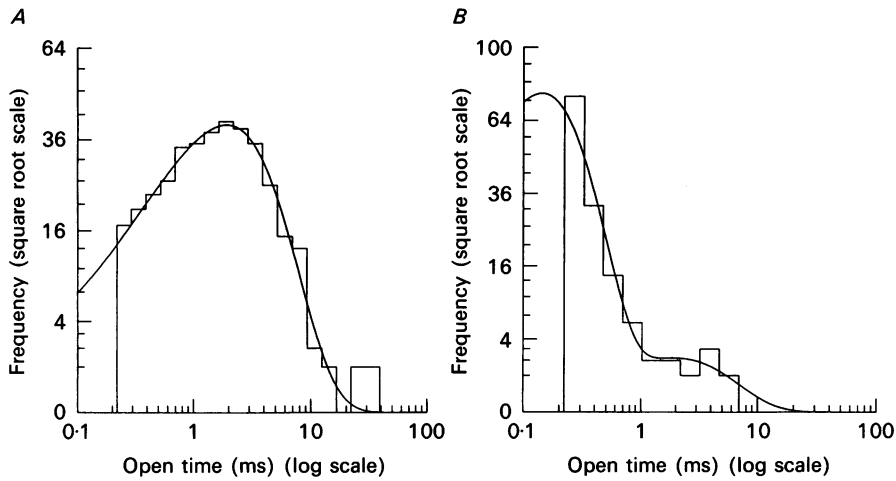

Fig. 6. Distributions of the lengths of apparent openings conditional on the amplitude of the openings. The amplitude distribution from this recording was constructed from 481 openings which were longer than 0·22 ms ($2{\cdot}0t_r$) and was fitted with two Gaussian components with parameters of $2{\cdot}81 \pm 0{\cdot}48$ pA (25%) and $3{\cdot}99 \pm 0{\cdot}29$ (75%) giving an A_{crit} value (see Methods) of 3·37 pA as minimizing the overlap between these two components. Of these 481 openings, thirty-six were connected by direct transitions between the two levels. Eighteen transitions were from the low to high amplitude range and eighteen transitions were from the higher to lower amplitude range. *A*, the distribution shown is of 362 openings longer than 0·22 ms ($2{\cdot}0t_r$) with amplitudes in the large amplitude class (3·37–5·5 pA). This distribution was fitted with the sum of two exponential components of 0·31 ms (10%) and 2·07 ms (90%). The fit predicts that there are 419 openings in this class in the data record. *B*, distribution of 119 open times longer than 0·22 ms with amplitudes in the range 1·0–3·37 pA. The distribution is fitted over the range of 0·22–10 ms with two exponential components with parameters of 0·14 ms (97%) and 1·78 ms (3%). The fit predicts that there are 542 openings in this class in the data record.

those to the secondary conductance level). Openings were assigned as 'full' or 'sublevel' using an A_{crit} value calculated from the fit to the amplitude distribution as described in Methods. Short openings (less than $2t_r$, 110–330 μs) were not included in these distributions.

In nineteen patches where two or more components were evident in the amplitude distribution, distributions of all open times longer than $2t_r$ were fitted with two exponential components of $0{\cdot}38 \pm 0{\cdot}05$ ms (61 ± 5%) and $3{\cdot}62 \pm 0{\cdot}51$ ms (39 ± 5%) (when short openings were excluded, generally a third component was not detectable). The distribution means averaged $1{\cdot}74 \pm 0{\cdot}28$ ms. Distributions of large conductance openings were also generally fitted with two exponential components (Fig. 6*A*) which averaged $0{\cdot}78 \pm 0{\cdot}13$ ms (47 ± 8%) and $3{\cdot}99 \pm 0{\cdot}59$ ms (53 ± 8%). The distribution means averaged $2{\cdot}62 \pm 0{\cdot}48$ ms. Distributions of sublevel openings

contained mainly a single fast component (Fig. 6*B*) and a much smaller slow component. The fitted parameters for the distributions of sublevel openings were 0·27 ± 0·04 ms (87 ± 4%) and 2·71 ± 0·65 ms (13 ± 4%). The distribution means averaged 0·52 ± 0·1 ms. Thus the mean duration of full openings is on average 5 times that of openings to other conductance levels.

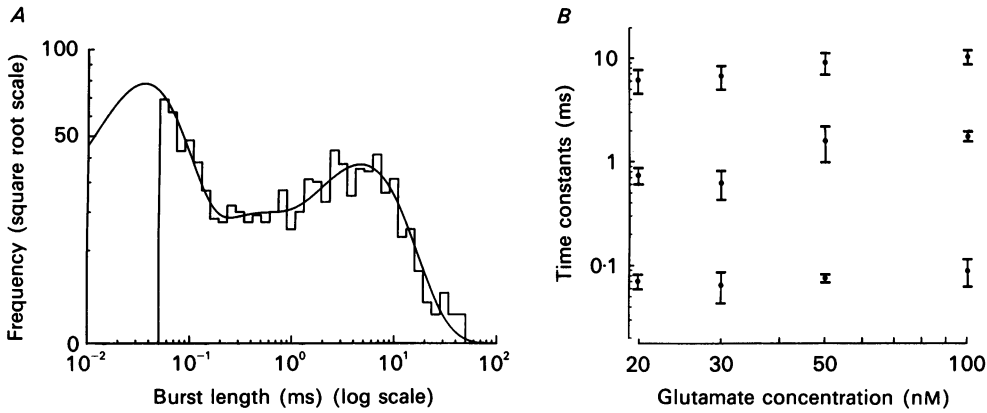

Fig. 7. *A*, distribution of burst lengths. The critical gap length was 0·46 ms. 897 bursts were identified between 50 μs and 50 ms long. The distribution is shown fitted with the sum of three exponential components. These had time constants (and relative areas) of: 34 μs (60%), 0·28 ms (10%), 4·59 ms (30%). The fitted curve predicts a total of 1740 bursts. *B*, double logarithmic plot of the mean time constants of the burst length distributions as a function of glutamate concentration. Points shown are the mean ± S.E.M. of the results from five to eight different patches at each concentration.

Burst length distribution

It is useful to define bursts of openings in the data record, because, even apart from the light this may cast on receptor mechanisms, the duration of these bursts is likely to be much less affected than are open time durations by the fact that short events are missed (see above). Bursts were defined empirically to include all gaps shorter than a critical gap length, t_c. The value of t_c was calculated (see Methods) between τ_2 and τ_3, the 2nd and 3rd closed time components (the mean t_c was 1·85 ± 0·4 ms). The definition of bursts is imperfect in so far as the approximately tenfold ratio between τ_2 and τ_3 is not quite as big as would be desirable for unambiguous classification of shut times as being 'within' or 'between' bursts. Distributions of burst lengths could be fitted well with the sum of three exponential components (Fig. 7*A*). These had mean time constants (and relative areas) of 76 ± 8 μs (53 ± 4%), 1·1 ± 0·17 ms (25 ± 3%) and 7·69 ± 0·9 ms (22 ± 3%) with a distribution mean of 2·3 ± 0·4 ms. These burst distribution characteristics are similar to those which have been previously described for recordings of NMDA receptor channel activity (Howe *et al.* 1988, 1991; Ascher, Bregestovski & Nowak, 1988; Cull-Candy & Usowicz, 1989; Traynelis & Cull-Candy, 1991).

There was no clear indication that the characteristics of the burst length distributions were dependent on glutamate concentration. Figure 7*B* shows the burst

length distribution time constants plotted against glutamate concentration. Over this limited glutamate concentration range, they change little. The relative area of the fast component decreased slightly with increasing agonist concentration (as is observed for muscle type nicotinic receptors; Colquhoun & Sakmann, 1985). There

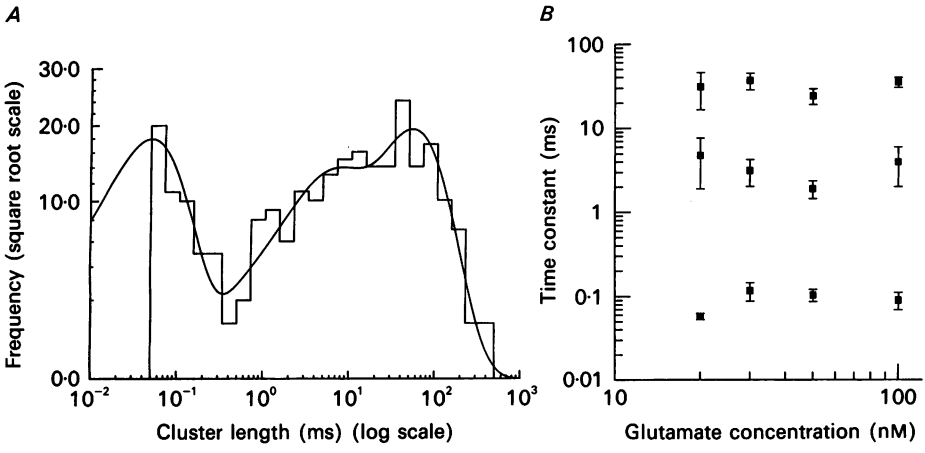

Fig. 8. *A*, distribution of the length of 244 clusters that were identified using a critical gap length of 28·3 ms. The distribution is shown fitted with the sum of three exponential components with time constants (and areas) of 50 μs (39%), 4·6 ms (19%), 54·5 ms (42%). The fit predicts that there were a total of 324 clusters in the data record. *B*, double logarithmic plot of the mean time constants of the cluster length distributions as a function of glutamate concentration. Points shown are the mean $\pm$ S.E.M. of the results from four different patches at each concentration.

was also some indication that the time constant and relative area of the slow component of the burst length distribution increased with agonist concentration. However, variation in the area of the burst length intermediate component tends to obscure any relationship between the glutamate concentration and the areas of the fast and slow components.

Distribution of the duration of clusters of bursts

It is clear from inspection of the recording in Fig. 3 that groupings of openings occur that contain shut times longer than the t_c value (mean 1·85 ms) used to define bursts, and it has already been suggested that the evidence favours the view that the third shut time component, $\tau_3 = 7{\cdot}56$ ms, also represents shut periods that occur within a single receptor activation. In an attempt to define more closely the individual activations we therefore now define *clusters* of openings in the data record using a critical gap length calculated between components 3 and 4 of the shut time distributions (the mean t_c was $16{\cdot}4 \pm 1{\cdot}9$ ms). Whether clusters so defined represent individual channel activations depends on whether the fourth shut time component, $\tau_4 = 137$ ms, should also be regarded as occurring 'within activations'; this question is considered when 'super-clusters' are discussed, below.

An example of the distribution of the length of such clusters is shown in Fig. 8*A*. Distributions of cluster lengths were fitted with three exponential components for

sixteen patches which contained enough data to allow cluster measurement. These distributions averaged 88 ± 10 μs (area 45 ± 5%), $3{\cdot}4 \pm 0{\cdot}9$ ms (25 ± 4%) and $31{\cdot}7 \pm 4{\cdot}3$ ms (30 ± 4%) with a distribution mean of $11{\cdot}5 \pm 1{\cdot}8$ ms. There was no clear concentration dependence for any of the cluster length distribution parameters (Fig.

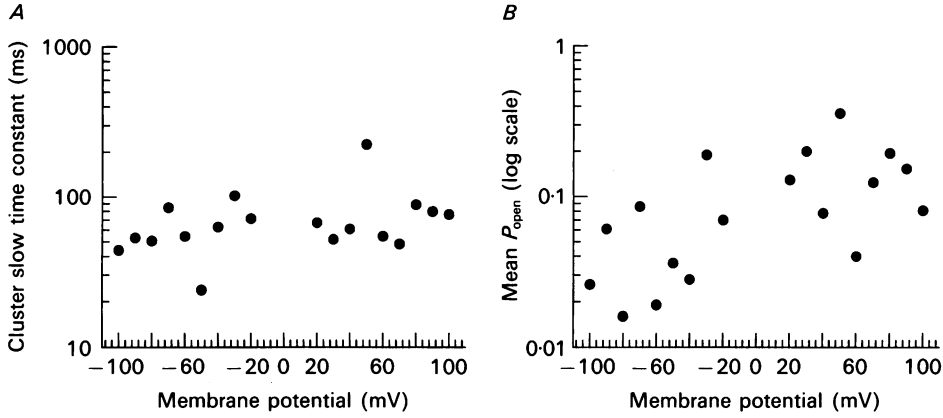

Fig. 9. *A*, absence of voltage dependence of the duration of NMDA channel activity measured at voltages between −100 and +100 mV. The plot shows the value of the slow time constant from the fit to the cluster length distributions plotted semilogarithmically as a function of patch potential. *B*, semilogarithmic plot of the mean P_{open} at each membrane potential.

8*B*) although, like the burst length distributions, the area of the fast component tended to be greater at lower agonist concentrations.

Voltage dependence of NMDA channel clusters

In most recordings it was not possible to record for prolonged periods at a wide range of membrane voltages. However, one patch where this was possible is illustrated in Fig. 9. Figure 9*A* shows a plot of the slowest time constant from the cluster length distributions measured over the range from −100 to +100 mV. In this patch there was no clear evidence for any voltage dependence of the NMDA cluster length. This is of interest with regard to the findings of Keller *et al.* (1991) who observed that the decay of the NMDA component of EPSCs in hippocampal granule cells is clearly voltage dependent. They observed that this voltage dependence was at least partly dependent on extracellular Mg^{2+}, so it may not be evident in this study where the concentration of extracellular divalent cations has been buffered to very low levels. However, as is evident from Fig. 9*B*, the mean channel open probability, P_{open}, measured over the whole data record, tended to increase in this patch when going from negative to positive potentials. For example, in this case there was an average P_{open} of $0{\cdot}059 \pm 0{\cdot}018$ at negative potentials and an average P_{open} of $0{\cdot}12 \pm 0{\cdot}02$ at positive potentials. This increase in P_{open} at positive potentials was almost entirely accounted for by the increase in the frequency of apparent openings from $15{\cdot}1 \pm 3{\cdot}35$ s^{-1} at negative potentials to $25{\cdot}9 \pm 5{\cdot}81$ s^{-1} at positive potentials. This effect is unlikely to be due to run-down or run-up of channel activity during

recording since stability plot analysis of NMDA channel activity (Gibb & Colquhoun, 1991) shows little sign of non-stationarity suggesting that the observed voltage dependence is not due to this.

Distribution of the total open time per burst

In principle the number of components in the distribution of total open time per burst should be the same as the number of components in the distribution of apparent open times, which is equal to the number of open states in the system (Colquhoun & Hawkes, 1981, 1982). It is therefore of interest to examine distributions

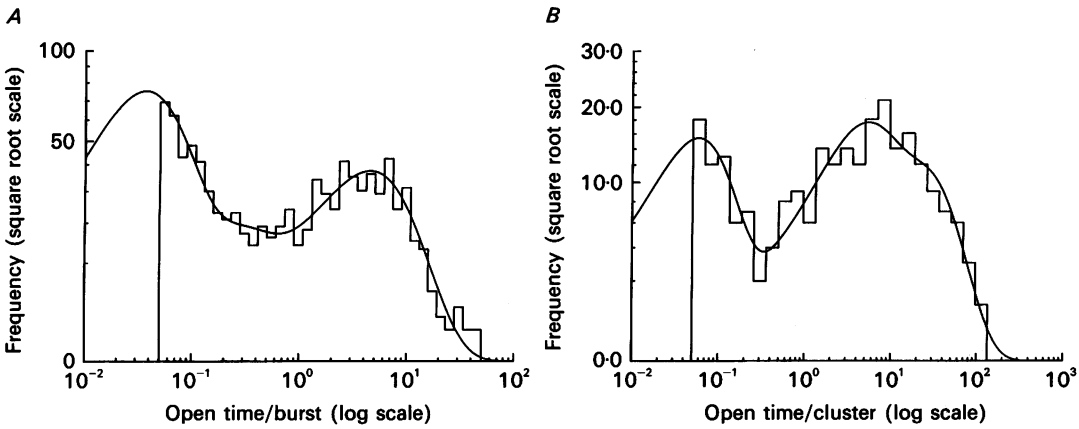

Fig. 10. *A*, distribution of the total open time per burst for the same patch as shown in the burst length distribution of Fig. 7. 597 bursts were included in the histogram which was fitted with three exponential components of 34 μs (57%), 0·19 ms (12%) and 4·48 ms (31%). The fit predicts that there are 1697 bursts. *B*, distribution of the total open time per cluster. Clusters were defined as for Fig. 8*A*. The distribution of the total open time for 244 clusters was fitted with the sum of three exponential components with time constants (and areas) of 56 μs (39%), 3·85 ms (31%) and 21·0 ms (30%) and predicted 318 clusters in total.

of the total open time per burst for each patch, because this distribution is much less susceptible to errors resulting from missed brief shuttings than is the distribution of apparent open times. Distributions of total open time per burst were fitted with three exponential components, as illustrated in Fig. 10*A*. From all patches analysed these had mean time constants (and relative areas) of 78 ± 9 μs (53 ± 4%), $1{\cdot}05 \pm 0{\cdot}23$ ms (25 ± 4%) and $6{\cdot}84 \pm 0{\cdot}72$ ms (22 ± 4%). The distribution means averaged $2{\cdot}02 \pm 0{\cdot}37$ ms. Both the time constants and the relative areas of these components were very similar to those of the burst length distribution, as expected when the gaps within bursts are relatively short.

The fraction of time for which the channel is open during a burst (the burst P_{open}) can be calculated by from the ratio of the mean total open time per burst to the mean burst length. The average burst P_{open} was $0{\cdot}86 \pm 0{\cdot}03$.

The total open time per cluster

Distributions of the total open time per cluster could also be fitted with three

exponential components (Fig. 10*B*) suggesting that there are three open states contributing to activity during clusters. The mean time constants (and relative areas) of these components were 122 ± 23 μs (43 ± 5%), $2{\cdot}78 \pm 0{\cdot}62$ ms (34 ± 4%) and $21{\cdot}9 \pm 3{\cdot}8$ ms (24 ± 4%).

The mean probability of being open during a cluster, P_{open}, can thus be estimated from the mean total open time per cluster divided by the mean length of all clusters giving a mean cluster $P_{open} = 0{\cdot}62 \pm 0{\cdot}11$.

Super-clusters

In outside-out patches, only the longest component (τ_5) of the shut time distribution shows a clear dependence on glutamate concentration (Gibb & Colquhoun, 1991). Thus even component 4 ($\tau_4 = 137$ ms here) could represent shut times that occur within individual receptor activations (the possible nature of such shut times is considered in the Discussion). The evidence that this is the case is not so strong as the evidence demonstrating that shut-time components 1, 2 and 3 represent gaps within activations; in order to be quite certain about this point it would be necessary to have records of a few thousand openings with at least 10 s, on average, between activations; such very long records are not easy to obtain. Nevertheless, it is clear from our data that even at these low glutamate concentrations groups of openings, which we term 'super-clusters' (Gibb & Colquhoun, 1991) can be defined which include gaps underlying component 4 of the shut time distribution.

Super-clusters were defined using a critical gap length, t_c (mean length 169 ± 33 ms), calculated between components 4 and 5 of the shut time distributions. Distributions of the lengths of these clusters were fitted with three exponential components with time constants (and relative areas) of $0{\cdot}16 \pm 0{\cdot}05$ ms (34 ± 6%), $3{\cdot}96 \pm 0{\cdot}85$ ms (16 ± 3%) and 166 ± 24 ms (51 ± 5%). The first two components have time constants similar to the first two components of the cluster length distribution (Table 1). The overall mean super-cluster length (calculated as $\Sigma a_i \tau_i$ from the fitted distributions) was 90 ± 17 ms, while the mean total open time per super-cluster was $16{\cdot}8 \pm 4$ ms giving an average P_{open} during these clusters of $0{\cdot}20 \pm 0{\cdot}05$.

Distributions of the number of apparent openings per burst

In principle, if three exponential components are present in the distribution of open times and in the distribution of total open time per burst, then there should also be three geometric components in the distribution of the number of openings per burst (Colquhoun & Hawkes, 1982). However, in practice components may be missed if they are too small to be clearly detected or if they have a mean that is close to that of another component. In these experiments only two geometric components were detectable in the distribution of the number of apparent openings per burst (Fig. 11*A*). These had mean values of $1{\cdot}15 \pm 0{\cdot}03$ (area 63 ± 5%) and $2{\cdot}71 \pm 0{\cdot}19$ (37 ± 5%) openings per burst. The distribution means averaged $1{\cdot}72 \pm 0{\cdot}08$ apparent openings per burst (this does not, of course, include missed events). The proportion of all observed bursts that consist of one apparent opening, $P(1) = \Sigma a_i/\mu_i = 0{\cdot}68$ (where a_i and μ_i are the area and mean for the ith component, e.g. Colquhoun & Sigworth, 1983).

Number of apparent openings per cluster

Distributions of the number of openings per cluster were fitted with three geometric components (Fig. 11*B*). These had mean values (and relative areas) of 1·22±0·04 (37±4%), 3·19±0·38 (44±5%) and 11·0±1·6 (19±5%). The overall mean is 3·56±0·39 apparent openings per cluster, which implies an average of 3·56/1·72 = 2·07 bursts per cluster (not corrected for missed events), or 11/1·72 = 6·4 bursts per 'long cluster' (i.e. clusters that underlie the long component of the cluster length distribution).

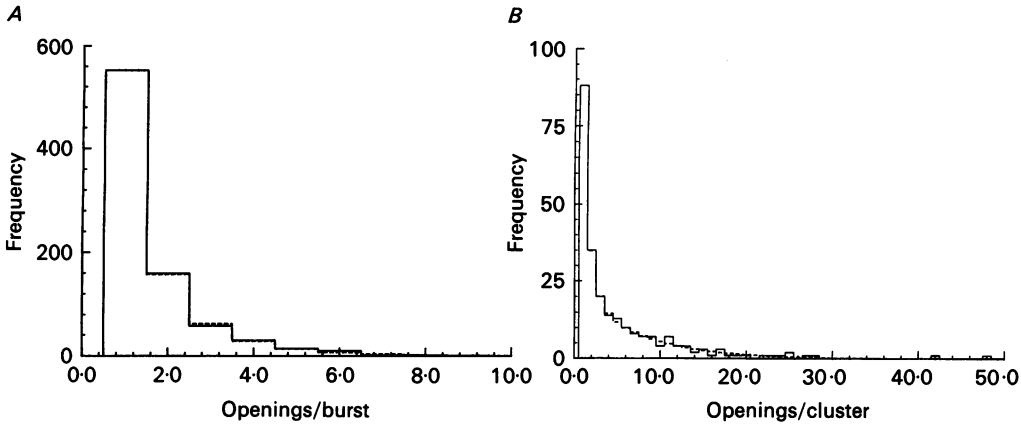

Fig. 11. *A*, distribution of the number of apparent openings per burst fitted with two geometric components. The distribution is for the same patch as analysed in Fig. 7. The fitted geometric components are shown as dashed bins superimposed on the data. The components of the fit had means of 1·06 (27%) and 1·91 (73%) openings per burst. *B*, distribution of the number of apparent openings per cluster, for the same data as described in Fig. 8. The distribution was fitted with the sum of three geometric components (shown as dashed bins) to clusters with between 1 and 30 apparent openings. The fitted parameters were 1·2 (19%), 1·6 (19%) and 7·5 (61%) openings per cluster.

The first two components in this distribution have mean values close to the corresponding components of the number of openings per burst distribution (see Table 1), which suggests that these components reflect clusters that consist of single openings and of single isolated bursts, respectively. The proportion of all observed clusters that consists of one apparent opening, $P(1) = 0{\cdot}61$, so the *number* of clusters with one opening is substantially less than the number of bursts with one opening. Thus some of the openings which appear as single isolated openings in the burst distributions are in fact part of multi-opening clusters (i.e. clusters that do not consist *only* of one short opening).

The length of apparent openings in bursts of a specified number of openings

It is noticeable that the first two time constants of the distribution of individual apparent open times (87±9 μs, 0·91±0·16 ms) are very similar to the first two time constants of the burst length (76±8 μs, 1·1±0·17 ms) and of the total open time per burst (84±8 μs, 1·17±0·24 ms) distributions (see Table 1). This suggests, in

agreement with the presence of only two components in the distribution of the number of openings per burst, that these first two components represent mainly single apparent openings which occur in the data record separated by gaps that are longer than the critical gap length used to define bursts (mean value $t_c = 1{\cdot}85$ ms);

TABLE 1. Summary of distribution parameters

Component	1 (μs)	2 (ms)	3 (ms)	4 (ms)	5 (ms)	Distribution mean (ms)
Shut time	68±7	0·72±0·12	7·56±0·8	137±26	922±195	192±48
	38±3%	12±2%	17±2%	22±4%	18±3%	
Apparent open time	87±9	0·91±0·16	4·72±0·6	—	—	1·22±0·2
	51±4%	31±3%	18±3%			
All openings $> 2t_r$	—	0·38±0·05	3·62±0·51	—	—	1·74±0·28
		61±5%	39±5%			
'50 pS' openings $> 2t_r$	—	0·78±0·13	3·99±0·59	—	—	2·62±0·48
		47±8%	53±8%			
Sublevel openings $> 2t_r$	—	0·27±0·04	2·71±0·65	—	—	0·52±0·1
		89±4%	12±4%			
Openings in bursts with 1 opening	81±11	0·82±0·14	4·42±0·56	—	—	1·14±0·24
	57±4%	27±4%	16±3%			
Openings in bursts with > 1 opening	107±16	1·11±0·22	4·55±0·56	—	—	1·87±0·34
	45±4%	25±4%	30±4%			
Burst length	76±8	1·1±0·17	7·69±0·9	—	—	2·30±0·4
	53±4%	25±3%	22±3%			
Total opening per burst	78±9	1·05±0·23	6·84±0·77	—	—	2·02±0·37
	53±4%	25±4%	22±4%			
Cluster length	88±10	3·4±0·9	31·7±4·3	—	—	11·5±1·8
	45±5%	25±4%	30±4%			
Total opening per cluster	122±23	2·78±0·62	21·9±3·8	—	—	6·66±1·3
	43±5%	34±4%	24±4%			
Super-cluster length	161±47	3·96±0·85	166±24	—	—	90±17
	34±6%	16±3%	51±5%			
No. of apparent openings per burst	1·15±0·03	2·71±0·19	—	—	—	1·72±0·08
	63±5%	37±5%				
No. of apparent openings per cluster	1·22±0·04	3·19±0·38	11·0±1·6	—	—	3·56±0·39
	37±4%	44±5%	19±5%			
Burst P_{open}	0·86±0·03					
Cluster P_{open}	0·62±0·11					
Super-cluster P_{open}	0·2±0·05					

Measurements of the distribution parameters obtained from the analysis of NMDA channel activity at low glutamate concentrations. Shown is the mean±S.E.M. of each parameter and immediately below each parameter estimate is given the mean±S.E.M. of the percentage area of that component.

in other words they appear to constitute bursts that contain only one apparent opening. The distribution of the number of openings per burst does indeed contain a component with a mean close to one opening per burst (actually 1·15 openings per burst). However, the number of observed openings which underlie the first two components of the open time distributions (calculated by integrating each component from the open time resolution to infinity) was on average 359±41 ($n = 19$ patches) whereas the number of single opening bursts was 215±30 on average (calculated from $N_b P(1) = N_b \Sigma a_i/\mu_i$ where N_b = total number of bursts). Thus not all of those

openings which underlie the first two components of the apparent open time distribution are bursts with only one opening; some of them must occur *within* multiple opening bursts.

In contrast, the numbers of observations underlying the first two components of the burst length and total open time burst distribution were 189 ± 26 and 191 ± 27

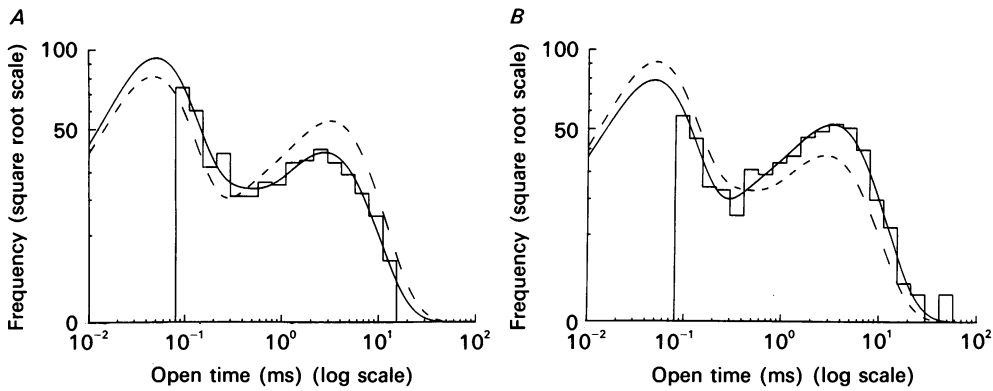

Fig. 12. Distribution of the duration of apparent open periods conditional on the number of apparent open periods in the burst. *A*, the distribution of the length of 511 bursts which were composed of a single open period. The continuous line shows the fit to the distribution of three exponential components with parameters of 46 μs (61%), 0·19 ms (11%) and 2·77 ms (28%). The fit predicts a total of 1139 open periods. The dashed line shows a copy of the fitted line in *B* scaled so that it includes the same number of events as the continuous line in *A*. The difference between dashed and continuous lines illustrates that relative to the distribution of open periods in bursts of more than one apparent opening (*B*), bursts of only one apparent opening contain relatively more short openings and relatively less long openings. *B*, the continuous line shows the fitted curve to 570 open periods in bursts of more than one apparent opening. The fitted parameters were 45 μs (50%), 0·37 ms (4·6%) and 3·24 ms (40%). The fit predicts a total of 1104 open periods. The dashed line shows a copy of the fitted line in *A* scaled so that it includes the same number of events as the continuous line in *B*.

respectively suggesting (since these numbers are close to the 215 ± 30 single opening bursts predicted from the distribution of the number of openings per burst) that the first two components in the burst length distribution represent mainly single openings.

To test these inferences we have constructed distributions of the lengths of open periods (*a*) in bursts with only one apparent open period, and (*b*) in bursts with more than one apparent open period. An *open period* is defined as a period of time during which the channel appears to be continuously open; open periods may contain more than one apparent opening when there is a direct transition between conductance levels (open periods are used here, rather than openings, as bursts are defined according to the length of the gaps between open periods. Thus the number of shut periods per burst is always one less than the number of open periods).

Examples of these distributions are shown in Fig. 12. The open times used in Fig. 12 are the same open times as used to construct the unconditional distribution shown in Fig. 5. Relative to the unconditional distribution, the distribution of open periods

in bursts that have only one apparent opening (Fig. 12*A*) contains a smaller slow component and larger intermediate and fast components. In contrast the distribution of open periods in bursts composed of more than one open period (Fig. 12*B*) has smaller fast and intermediate components and a larger slow component (Table 1).

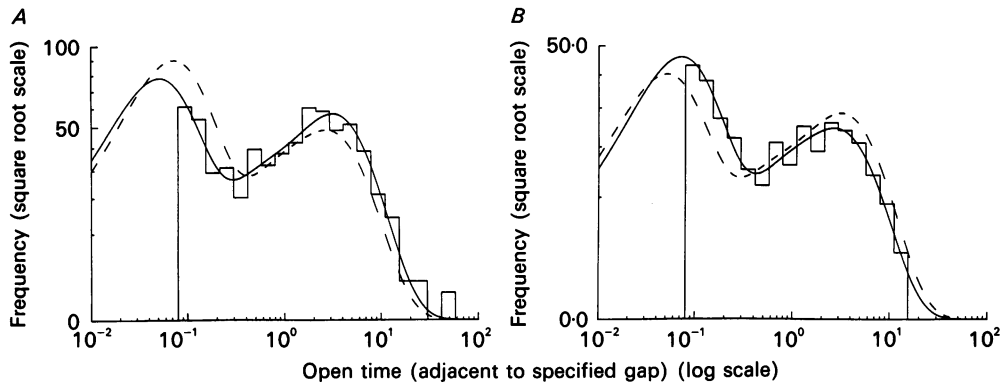

Fig. 13. Conditional distributions of apparent open times adjacent to brief (*A*) and long (*B*) shut times. *A*, from a total of 1206 apparent open times 640 were identified as adjacent to shut times in the range 50 μs to 0·3 ms. These were fitted with the sum of three exponential components (continuous curve) with parameters of 48 μs (52 %), 0·36 ms (8 %) and 3·21 ms (40 %). The fit predicted a total of 1154 open times. The dashed line in *A* shows the fit from *B* scaled to contain the same number of openings as the continuous line. *B*, a total of 335 open times were identified as adjacent to shut times in the range 50–5000 ms. These were fitted with the sum of three exponentials (continuous curve) with parameters of 68 μs (60 %), 0·46 ms (5·8 %) and 2·79 ms (35 %) which predicts a total of 590 open times. The dashed line shows the fit from *A* scaled to contain the same number of openings as in the continuous line. The difference between dashed and continuous lines indicates that relative to openings adjacent to long shut periods, there are more long openings and fewer short openings adjacent to short shut periods.

For open periods in bursts of only one open period, the distribution parameters were 81 ± 11 μs (57 ± 4 %), $0{\cdot}82 \pm 0{\cdot}14$ ms (27 ± 4 %) and $4{\cdot}42 \pm 0{\cdot}56$ ms (16 ± 3 %) with a distribution mean of $1{\cdot}14 \pm 0{\cdot}24$ ms, whereas for open periods in bursts of more than one opening the distribution parameters were 107 ± 16 μs (45 ± 4 %), $1{\cdot}11 \pm 0{\cdot}22$ ms (25 ± 4 %) and $4{\cdot}55 \pm 0{\cdot}56$ (30 ± 4 %) with a distribution mean of $1{\cdot}87 \pm 0{\cdot}34$ ms. While the time constants of each component are not significantly different from each other in the two types of distribution, the relative areas of the fast and slow components are. In agreement with the results on the frequency of direct transitions between conductance levels, and also the adjacent interval analysis (see below) this result supports the idea that the channel gating has the properties of a Markov process.

It is clear that all three exponential components are present in each case. This confirms the suggestion that bursts with more than one apparent opening (and hence also clusters with more than one opening) in fact contain openings of all three 'types'. This situation is similar to that described for neuronal AChR channel openings in sympathetic ganglia (Mathie *et al.* 1991) but is different from muscle AChR activations where bursts with > 1 opening are composed of mainly long openings (Colquhoun & Sakmann, 1985; Sine & Steinbach, 1986).

Distributions of open times adjacent to gaps of specified length

Correlations between the length of one open time and the length of the following shut, or open, times, can provide valuable information about receptor mechanisms (Fredkin, Montal & Rice, 1985; Colquhoun & Hawkes, 1987). Blatz & Magleby (1989)

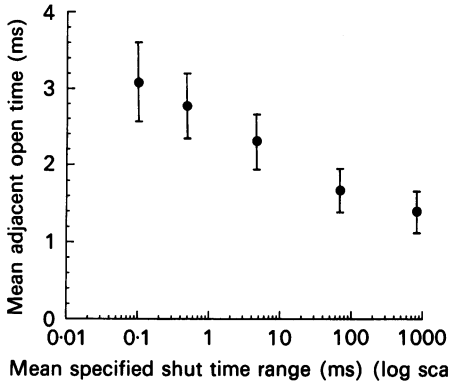

Fig. 14. Relationship between the mean durations of adjacent open and shut intervals. The graph shows the mean ± S.E.M. of the open times in sixteen different patches plotted against the average of the mean adjacent shut time ranges used in each patch.

and McManus & Magleby (1989) have demonstrated the advantages of using distributions of adjacent intervals as a means of examining the strength of any correlations between open times and closed times in a single channel data record. The principles of the analysis of open times adjacent to closed times of a particular length are illustrated by the results shown in Fig. 13. Figure 13*A* shows the distribution of open times adjacent to closed times in the range 50 μs to 0·5 ms. These data are from the same patch as used to construct the unconditional open time distribution shown in Fig. 5. Relative to the distribution of unconditional open times, the distribution of open times adjacent to short closed periods contains a larger slow component and a smaller fast component. In contrast, the distribution of open times in the same recording adjacent to closed periods in the range 50–5000 ms (Fig. 13*B*) shows a larger fast component and smaller slow component than the unconditional open times distribution.

This general picture relating changes in open time distribution component areas to the lengths of adjacent closed periods was consistently seen. In contrast the time constants of the fitted conditional distributions did not change consistently with changing adjacent gap length. The main difficulty with applying this method of analysis in the present case was that in some patches there were not enough observations in the distributions of adjacent open times to give accurate estimates of all fitted parameters. This difficulty was addressed by Blatz & Magleby (1989) who used the *mean* open time adjacent to closed times in a particular range, rather than attempting to construct the whole distribution of such open times. The results of this approach are shown in Fig. 14 where the mean open times adjacent to specified closed time ranges are shown plotted against the mean of each closed time range. The graph

shows the averages of the mean open times from sixteen different patches. It is clear that there is an inverse relationship between open times and adjacent closed times; in other words there is a negative correlation between open times and closed times in the data.

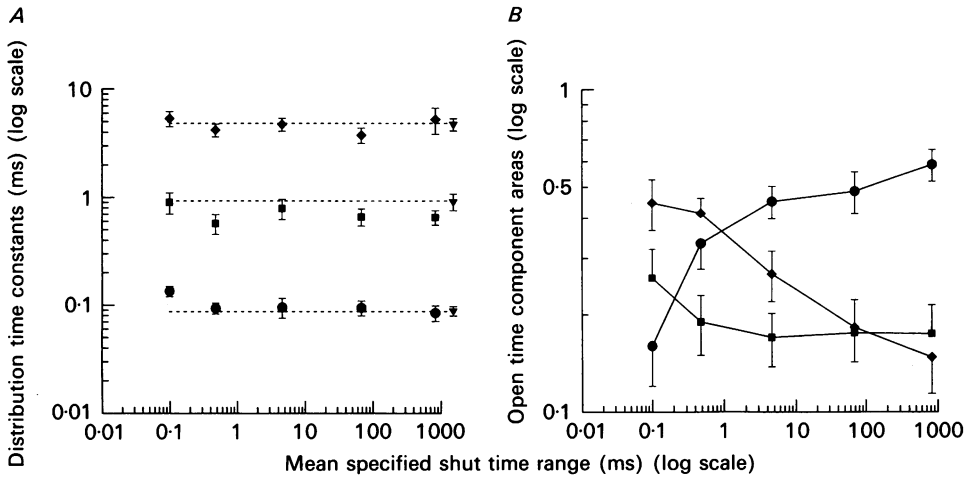

Fig. 15. Mean time constants (*A*) and areas (*B*) of the exponential components describing conditional open time distributions from sixteen different patches. The mean ± S.E.M. for each fitted parameter is shown plotted against the average of the mean adjacent shut time ranges used in each path. The inverted triangles to the right of the data values in *A* show the mean ± S.E.M. of the time constants from the unconditional open time distributions and the dashed lines show the position of each mean across the plot. In *B*, ●, ■ and ◆ refer to the area of the fast, intermediate and slow components of the open time distributions. The lines drawn in *B* have experimental values only at the data points and are drawn only so that the data values for each open time component can be clearly identified.

The distributions of adjacent open intervals from each of these sixteen different patches were fitted with three exponential components and the results are summarized in Fig. 15. In Fig. 15*A* the mean time constants for each component are plotted against mean adjacent closed time range. The results suggest that there is no significant change in the time constants of the open time distributions with changes in adjacent closed time range. In contrast (Fig. 15*B*) there is a clear increase in the area of the fast component and a concomitant decrease in the area of the slow component with increasing adjacent closed time interval. Apart from the shortest closed time range, the area of the intermediate component is approximately 20% at all closed time ranges.

Although the relative area of the fast and slow components in these conditional open time distributions changed considerably with changing adjacent closed time range, all three components are clearly present at each closed time range examined, suggesting a close connectivity between the three expected open states and their adjacent shut states. The data summarized in Fig. 15 are from sixteen patches with channels activated by 20, 30, 50 and 100 nM-glutamate. However, examination of the

data at each individual glutamate concentration shows no obvious trend related to glutamate concentration in the adjacent interval analysis which could have enhanced the correlations observed here. In addition, although the effects of limited time resolution may change the magnitude of any observed correlation, limited time resolution is unlikely to generate an artifactual correlation (Ball & Sansom, 1988).

DISCUSSION

The results presented in this paper describe the properties of the ion channel openings which occur on activation by glutamate of NMDA receptors in cells dissociated from adult rat hippocampus. As in the case of the AChRs from muscle (Colquhoun & Sakmann, 1981, 1985; Sine & Steinbach, 1986) or electric organ (Sine *et al.* 1990) or the glutamate receptor of locust muscle (Cull-Candy & Parker, 1982), a single activation of the NMDA receptor can produce multiple channel openings. However, unlike the AChR, where each activation consists predominantly of a single burst of closely spaced openings, activation of the NMDA receptor produces several bursts which are grouped together as a long cluster.

Activations of the NMDA receptor

Figure 16 shows an attempt to represent diagrammatically the average characteristics of channel openings generated by a single activation of the endplate AChR and the NMDA receptor, though it is hard to convey an accurate description of a stochastic process in this way. Activation of endplate receptors by ACh generates either single 'short openings', (this expression is used to denote the component of the distribution with $\tau = 140$ μs) or bursts of 'long openings' ($\tau = 1{\cdot}4$ ms) separated by 'short gaps' ($\tau = 20$ μs), the latter being the physiologically important response. In contrast activation of NMDA receptors by glutamate may produce 'short openings' ($\tau = 90$ μs), 'intermediate openings' ($\tau = 0{\cdot}9$ ms), sublevel openings ($\tau = 0{\cdot}3$ ms) or 'long openings' ($\tau = 4$ ms). Openings of any duration can occur within bursts, where they are separated by 'short gaps' ($\tau = 70$ μs) or 'intermediate gaps' ($\tau = 0{\cdot}7$ ms). These bursts are quite like those seen with endplate receptors, having about three openings on average, though 'intermediate gaps' are more common in NMDA bursts. However, whereas the end of a burst signals the end of the AChR activation, NMDA receptor activation generates several bursts of openings grouped together in a cluster (overall average about 3 bursts per cluster, or 6 bursts per 'long cluster').

Comparison with previous studies of NMDA receptor channels

Shut time distributions

The brief shut periods within each burst of channel activity have two exponential components with time constants of 68 μs and 0·72 ms (comprising 38 and 12% of all shut times, respectively). These values are comparable with those found for the muscle-type nicotinic receptor (e.g. 20 μs gaps, and much rarer 0·51 ms gaps, for ACh in frog endplate at 11 °C; Colquhoun & Sakmann, 1985). Similar values have been found for glutamate activation of NMDA channels in explant culture of cerebellar granule cells (Howe *et al.* 1991), viz. 63 μs and 0·66 ms (46 and 15% relative areas). Most other studies have not reported the briefest shut time component; for example

Ascher *et al.* (1988) found 0·43 ms for short gaps in mouse cultured midbrain neurones, and Jahr & Stevens (1990) reported 0·5 ms for cultured hippocampal CA1 neurones (the resolution was not stated in these studies, but was probably at least 200 μs); for large cerebellar neurones in culture Cull-Candy & Usowicz (1989) mention the existence of similar brief shuttings.

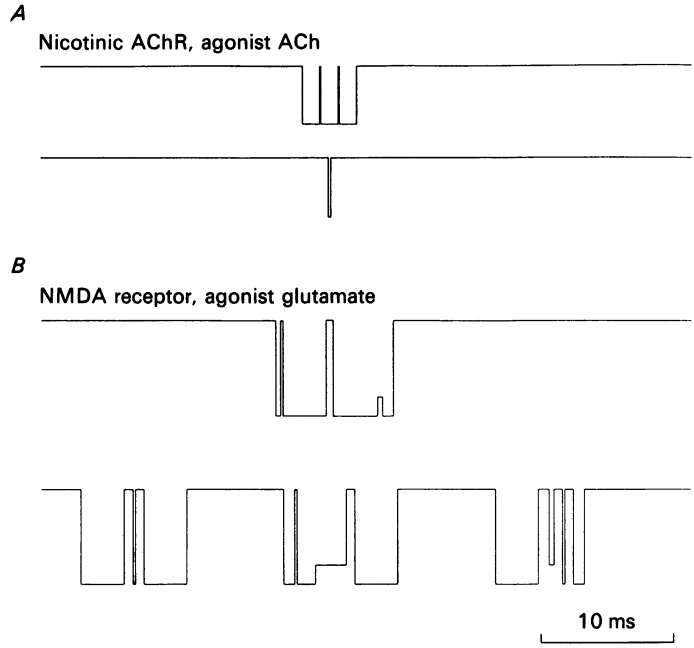

Fig. 16. Diagrammatical representation of the channel openings which result from activation of an endplate AChR when the agonist is ACh (*A*), compared with activation of the NMDA receptor by glutamate (*B*). *A*, activations characteristic of the endplate AChR. These take the form either of bursts (upper trace) which on average have three openings 1·4 ms long separated by 20 μs gaps, or receptor activation results in single short openings (lower trace) of around 0·14 ms duration. *B*, NMDA receptor activation causes single openings, bursts of around three openings (upper trace), or clusters of bursts (lower trace). Openings within each burst can be of 'short', 'intermediate' or 'long' duration, or subconductance openings. The gaps within each burst may be of 'short' (70 μs) or 'intermediate' (0·7 ms) duration. Clusters are composed of three bursts on average separated by gaps of around 8 ms duration (or six bursts per 'long cluster').

A notable point is that previous analyses of NMDA channel activity have not reported a shut time component with a time constant of around 10 ms. These intermediate-duration shut times were identified in this study as separating bursts within clusters. Few shut time distributions have been published in sufficient detail to show whether this is a real difference between the NMDA channel activity observed in these adult hippocampal cells and that observed in cultured cells or in explant cultures of cerebellar granule cells (Howe *et al.* 1991; Traynelis & Cull-Candy, 1991). Furthermore most previous studies used much higher agonist concentrations (1–100 μM) in the absence of added glycine. Thus it is not possible to be sure whether there is any fundamental difference between the NMDA receptors expressed in the

adult hippocampal cells and those examined in previous studies. The shut times observed in cell-attached or inside-out patches from these dissociated adult cells are, however, very similar to those observed in outside-out patches from CA1 cells in thin slices of hippocampus (Gibb & Colquhoun, 1991; Gibb & Edwards, 1991).

Bursts of openings

The characterization of bursts is of use, both in terms of considering the mechanism of NMDA receptor activation, and because previous studies have used bursts as the main measure of NMDA receptor activity. However, it is clear from this study that bursts do not represent single NMDA receptor activations and that in fact, many receptor activations generate several bursts which are grouped together as a cluster. Bursts were identified as including the first two gap components and distributions of the lengths of bursts were constructed. For the dissociated adult hippocampal cells these had time constants of 76 μs, 1·1 ms and 7·7 ms (relative areas 53, 25 and 22%, using a t_c = 1·85 ms) which compares with 8·5 ms (using a t_c = 1–10 ms; Ascher *et al.* 1988), 1·8 ms and 10·7 ms (using a t_c = 2·2 ms; Cull-Candy & Usowicz, 1989), 1·74 and 10·6 ms (using a t_c = 1–2 ms; Howe *et al.* 1991) and 46 μs, 1·0 ms and 6·02 ms (using a t_c = 2·5 ms; Traynelis & Cull-Candy, 1991). Both intermediate and slow components in the burst length distributions of Howe *et al.* (1991) were shown to result from openings to the 50 pS level, whereas here we find that a significant part of the intermediate component represents openings to the '40 pS' subconductance state (see also Ascher *et al.* 1988).

Correlations

In this study we find a clear negative correlation between the duration of open times and closed times in the data record. There was also a positive correlation between shut times and a positive correlation between open times. In contrast Jahr & Stevens (1990) found no correlations between closed times in their study of NMDA-activated channels in outside-out patches from cultured hippocampal cells. Thus their data would not be expected to show any correlations between open times and shut times either (Colquhoun & Hawkes, 1987; eqns 2.17 and 2.20). However, their study identified only one open state (rather than three here), and only three components in the shut time distribution, the resolution in their study being such that our shortest component could not have been detected. It is therefore likely that differences in resolution (or possibly differences between cell types) are the main reason for the differences between this study and that of Jahr & Stevens (1990).

High P_{open} periods

In this study, and in that of Gibb & Colquhoun (1991), long high P_{open} periods were evident in the data. Both Jahr & Stevens (1987) and Howe *et al.* (1988, 1991) also describe these high P_{open} periods (they were referred to as bursts and clusters respectively in these studies). Jahr & Stevens suggest that these high activity periods are associated with a 'long opening mode' of the NMDA receptor whereas Howe *et al.* (1988, 1991) and Gibb & Colquhoun (1991) found that openings within, or outside the high P_{open} periods were similar. As in the study of Howe *et al.* (1991), we find that the distribution of gaps within these high P_{open} periods consists mainly of gaps which

underlie the first two components in the shut time distribution. Unlike the clusters identified in this study, high P_{open} periods do not contain a gap component equivalent to the 8 ms gaps which separate bursts within a cluster. Thus the high P_{open} periods are like a very prolonged burst of openings but are rather different from the clusters of channel openings which result from most NMDA receptor activations.

The experiments of Jahr & Stevens (1987) and Howe *et al.* (1988, 1991) were in the presence of extracellular Ca^{2+}, without any added extracellular glycine and used agonist concentrations greater than 1 μM. These conditions are quite different from the low extracellular divalents, high glycine concentration and low glutamate concentration used in this study. In particular, the difference in glycine concentrations could have resulted in the clustering observed in this study. However, experiments in outside-out patches made from thin slices of hippocampus suggest that clustering at low glutamate concentrations is not dependent on the presence of relatively high concentrations of extracellular glycine (Gibb & Edwards, 1991). In fact the results of Gibb & Edwards (1991) suggest that the main effect of increasing the glycine concentration is to increase the frequency of receptor activations (as originally suggested by Johnson & Ascher, 1987) without any change in the properties of individual receptor activations.

Interpretation of the shut time distribution

The distribution of shut times was fitted with five exponential components suggesting that the NMDA receptor can enter a minimum of five shut states (Colquhoun & Hawkes, 1981, 1982). It is possible that the NMDA receptors in one patch are heterogenous, and if so this could contribute to the complexity of the shut time distribution (though it would not alter the qualitative conclusions concerning the length of individual activations). Macroscopic current recordings (Ascher *et al.* 1988; Lerma, Zukin & Bennett, 1990; Benveniste & Mayer, 1991) suggest that two agonist molecules must bind to the NMDA receptor to produce efficient receptor activation. Therefore, at least three closed states, unliganded, monoliganded and doubly liganded, are expected of the receptor. In addition the receptor has at least one binding site for glycine (Johnson & Ascher, 1987; Mayer *et al.* 1989; Lerma *et al.* 1990; Benveniste & Mayer, 1991). The present experiments were performed with the glycine concentration fixed at 1 μM. Since the equilibrium dissociation constant for glycine is of the order of 200 nM, with 1 μM-glycine this site should be occupied for most of the time. The existence of states with and without a glycine molecule bound will result in there being further shut states. In addition there is likely to be at least one desensitized state of the NMDA receptor (Mayer *et al.* 1989; Sather, Johnson, Henderson & Ascher, 1990; Lerma *et al.* 1990; Kiskin, Krishtal & Tsyndrenko, 1990). Thus in total these physical considerations suggest there are at least five closed states of the NMDA receptor. At present, however, there is little evidence to suggest which, if any, of these likely physical states underlies the components in the distribution of channel shut times.

However, the fastest three components in the closed time distribution are unlikely to reflect glutamate dissociation and reassociation. This is because the time constants of these three components do not change with glutamate concentration (see also Gibb & Colquhoun, 1991), they are consistent between patches which probably have different numbers of active channels, and, at these low glutamate concentrations,

most physically plausible values for the microscopic association rate of glutamate with the receptor suggest that agonist dissociation will result in gaps of 50 ms or longer in the data record.

If one assumes that glycine can associate and dissociate with any closed state of the receptor then at the 1 μM concentration of glycine used in this study the third closed time component (time constant 7·6 ms) could represent dissociation and reassociation of glycine with the receptor. However, experiments using recordings from outside-out patches where the glycine concentration was changed from 100 nM to 1 μM with no change in the time constants of the first three gap time components suggest that glycine unbinding and rebinding does not underlie this component in the closed time distribution (Gibb & Edwards 1991).

The presence of a component in the shut time distribution with an 8 ms time constant is of considerable interest because at these very low agonist concentrations gaps of this length are too short to be accounted for by agonist dissociation and reassociation. Consider, as an analogy, another potent agonist, suberyldicholine working on endplate nicotinic receptors: the mechanism, and rate constants, proposed by Colquhoun & Sakmann (1985) imply that, at a concentration of 30 nM, individual channel activations would be separated by an average shut time of 56037 ms. If a value of this order applied to the NMDA receptor, then there would have to be something of the order of 7000 channels in a single patch to generate the appearance of 8 ms gaps between individual activations (and all longer shut periods than this would have to be ascribed to desensitization). This is highly unlikely. This argument, together with the observed lack of dependence of the '8 ms' component on agonist concentration (Gibb & Colquhoun, 1991), suggests that these '8 ms gaps' occur within a single activation of the NMDA receptor. In contrast to the data on the three fastest closed time components, the two slowest closed time components vary between different patches and with glutamate concentration where two or more agonist concentrations have been tested on a single outside-out patch (see also Gibb & Colquhoun, 1991), suggesting that these may represent shut periods that include sojourns in states with zero or one agonist molecule bound to the receptor. As discussed by Gibb & Colquhoun (1991), the second slowest closed time component (mean 137 ± 26 ms) could also represent a short-lived desensitized state which would mean that each NMDA receptor activation could result in the clusters in the data record being grouped together into 'super-clusters'. If this were the case then the duration of the 'super-clusters' (slow component 166 ± 24 ms) would be expected to contribute to the decay of synaptic currents and could account for the small slow component evident in high resolution studies of NMDA receptor-mediated EPSCs (Lester *et al.* 1990; Hestrin *et al.* 1990*b*; Keller *et al.* 1991; Stern *et al.* 1992).

Evidence for multiple open states

Distributions of apparent open times were fitted with three exponential components. In addition three components were detected in the distribution of total open time per burst and in the distribution of total open time per cluster. This indicates that the NMDA receptor can enter a minimum of three different open states (Colquhoun & Hawkes, 1981, 1982). Distributions of channel amplitudes generally contained two significant components with a third component present in a few cases. This suggests at least two discrete open states. In some patches it seemed that the

intermediate component of the open time and burst length distributions was due mainly to openings to the main subconductance level (Fig. 6). However, on average the time constant of the intermediate component in the open time distribution ($0{\cdot}91 \pm 0{\cdot}16$ ms) is considerably longer than the time constant of the main component in the distribution of the durations of sublevel openings ($0{\cdot}27 \pm 0{\cdot}04$ ms) while the distribution of large amplitude openings contains a clear component with a time constant of $0{\cdot}78 \pm 0{\cdot}13$ ms. These results suggest there are at least two open states of large conductance and at least two open states of lower conductance.

Despite the fact that the short and intermediate components of the open time distribution represent a greater area than the slow component, openings which underlie the slow component of the open time distribution will contribute most of the membrane current recorded on activation of NMDA receptors because these openings have, on average, a much longer lifetime.

Discrete channel states and evidence for Markov gating

It is usually assumed that ion channel gating can be modelled by a finite number of discrete kinetic states with rate constants for transitions among these discrete states which are independent of previous channel activity. These discrete Markov models have been used to describe the gating of other ligand-gated channels such as the AChRs of muscle (Colquhoun & Sakmann, 1985; Sine & Steinbach, 1986) and electric organ (Sine *et al.* 1990) and of $GABA_A$ receptor channel activity in cultured chick neurones (Weiss & Magleby, 1989). The assumption of rate constants independent of previous channel activity was tested in this paper using the method of adjacent interval analysis (Blatz & Magleby, 1989; McManus & Magleby, 1989). This method uses the distributions of open times adjacent to shut times in a specified range, to test if the mean lifetime (and hence the underlying rate constants for transitions out of each open state) of open states is dependent on the adjacent closed period (previous channel activity). We find that the time constants (though not the relative areas) of the components of the conditional open time distributions are independent of previous channel activity, as expected for a discrete Markov mechanism.

The changes in the areas of each component in the adjacent open time distributions with changing adjacent shut time range result in a negative correlation between open times and their adjacent shut time. Similar negative correlations have been observed with the fast chloride channel in muscle (McManus, Blatz & Magleby, 1985) AChRs (Colquhoun & Sakmann, 1985; Sine & Steinbach, 1987), the large conductance calcium-activated K^+ channel in muscle (McManus & Magleby, 1986) $GABA_A$ receptor channels (Weiss & Magleby, 1989) and NMDA receptor channels in explant cultures of rat cerebellar granule cells (Howe *et al.* 1991).

The fact that there are correlations in the data indicates that there is more than one 'gateway' state between open states and closed states (Fredkin *et al.* 1985; Colquhoun & Hawkes, 1987). These correlations are evident in the conditional distributions of open times where the area of the fast component was greater for openings adjacent to long-lived shut times, while the area of the slow component was greater for openings adjacent to short shut times. Interestingly, except at short closed times, the area of the intermediate open time component, which includes most

of the subconductance openings, does not change significantly with changing adjacent closed time.

Additional information is provided by the presence of a component with near unit mean in the distribution of the number of openings per burst, and of the number of openings per cluster. A component with unit mean occurs when an open state is directly connected to a between-bursts shut state (or between-clusters shut state) and that open state is not a direct gateway state between open states and the within-bursts (or clusters) shut states (Colquhoun & Hawkes, 1987). For the NMDA channel activity analysed in this paper the component with near-unit mean in distributions of the number of openings per burst or per cluster seems to represent mainly short openings although both intermediate and long openings are also represented in this component (cf. distributions of open periods in bursts of one apparent opening; Fig. 12). Most subconductance openings occur as isolated openings in the distribution of burst lengths suggesting that these may not be directly connected to the within-burst shut states.

Comparison of NMDA channel gating with other channels

Functionally, NMDA receptors exhibit many similarities to other ligand-gated channels. In particular, the presence of closely interconnected multiple closed states and open states as suggested for AChRs (Colquhoun & Sakmann, 1985; Sine & Steinbach, 1986; Sine *et al.* 1990), for $GABA_A$ receptors (Weiss & Magleby, 1989; Twyman, Rogers & Macdonald, 1990) and for glycine receptors (Twyman & MacDonald, 1991) seems also to be the case for the NMDA receptor. However, it is also clear that the NMDA receptor has some unique properties, the most prominent of which is that the length of each receptor activation far exceeds that observed with the other ligand-gated receptor channels studied so far.

Receptor activation and the NMDA receptor-mediated synaptic current

The results of this study suggest that a single activation of the NMDA receptor produces a complex cluster of channel openings. The long gaps within each cluster may mean that activation of the NMDA receptor is a relatively slow process, which would be consistent with the slow rise time of the NMDA receptor-mediated component of synaptic currents (Hestrin *et al.* 1990*a*; Lester *et al.* 1990; Randel & Collingridge, 1991). Lester *et al.* (1990) and Hestrin *et al.* (1990*b*) have shown that the slow decay of the NMDA receptor-mediated EPSC is not due to diffusion and repeated binding of transmitter in the synaptic cleft, and have suggested, therefore, that the time course of the synaptic current is determined by channel gating. This conclusion has also been reached using numerical simulations of the NMDA receptor-mediated EPSC (Wathey, 1990). Furthermore, application of brief glutamate pulses to non-NMDA receptors suggests that the duration of the transmitter pulse in the synapse is, as at the neuromuscular junction, brief relative to the decay of synaptic currents (Colquhoun, Jonas & Sakmann, 1992).

We find that the duration of the clusters measured in this study (32 ms) and in a study using outside-out patches (Gibb & Colquhoun, 1991) is rather shorter than the synaptic current decay time constant although it is close to the time constant of the fast exponential component (40 ms) observed when two exponential components are

fitted to the decay of the NMDA EPSC in hippocampal slices (Keller *et al.* 1991; Randall & Collingridge, 1991) or in slices of visual cortex (Stern *et al.* 1992). On the other hand, the duration of the 'super-clusters' (defined using components 4 and 5 of the shut time distribution) is in the same range as most measurements of the NMDA receptor-mediated EPSC decay time constant. However, the evidence that gaps contributing to component 4 of the shut time distribution fall *within* receptor activations is less clear. Therefore the possibility that the 'super-clusters' (Gibb & Colquhoun, 1991) may determine the slow component of the synaptic current must remain speculative until further experiments are done.

At present it is uncertain whether the occasional high P_{open} periods in the data record are relevant to synaptic transmission. Because of the high P_{open} within these periods, each is almost certain due to a single activation of an NMDA receptor. However, high P_{open} periods occur at a very low frequency (around 1 or 2 per data record) suggesting that only rarely does a receptor activation generate this activity. Therefore, the significance of these events to synaptic transmission is uncertain, despite the fact that in steady-state recordings around 20% of all openings in the data record occur within these high activity periods (Gibb & Colquhoun, 1991).

In conclusion, the results of this study demonstrate that a single activation of the NMDA receptor can produce a long cluster of channel openings. The properties of these clusters give new insights into the channel activity underlying the NMDA component of EPSCs in the central nervous system. At present information is still lacking regarding the dependence of NMDA receptor single channel activity on glutamate concentration. However, it is now clear that the generation of the NMDA component of EPSCs is dependent on the NMDA channel kinetics (Hestrin *et al.* 1990*b*; Lester *et al.* 1990; Gibb & Colquhoun, 1991) and therefore knowledge of the concentration dependence of the NMDA receptor channel kinetics should allow predictions to be made of the kinetic behaviour which underlies the NMDA receptor-mediated EPSC.

We wish to thank Stuart Cull-Candy and Steve Traynelis for helpful comments on the manuscript, Mr A. T. Osborn for measuring the Mg^{2+} content of our solutions, and Jackie Carr for excellent technical assistance. This work was supported by the MRC and the Wellcome Trust.

REFERENCES

ASCHER, P., BREGESTOVSKI, P. & NOWAK, L. (1988). *N*-Methyl-D-aspartate-activated channels of mouse central neurones in magnesium-free solutions. *Journal of Physiology* **399**, 207–226.

ASCHER, P. & NOWAK, L. (1988). The role of divalent cations in the *N*-methyl-D-aspartate responses of mouse central neurones in culture. *Journal of Physiology* **399**, 247–266.

BALL, F. G. & SANSOM, M. S. P. (1988). Single channel autocorrelation functions: the effects of time interval omission. *Biophysical Journal* **53**, 819–832.

BENVENISTE, M. & MAYER, M. L. (1991). Kinetic analysis of antagonist action at *N*-methyl-D-aspartic acid receptors: Two binding sites each for glutamate and glycine. *Biophysical Journal* **59**, 560–573.

BLATZ, A. L. & MAGLEBY, K. L. (1986). Correcting single channel data for missed events. *Biophysical Journal* **49**, 967–980.

BLATZ, A. L. & MAGLEBY, K. L. (1989). Adjacent interval analysis distinguishes among gating mechanisms for the fast chloride channel from rat skeletal muscle. *Journal of Physiology* **410**, 561–585.

COLLINGRIDGE, G. L., HERRON, C. E. & LESTER, R. A. J. (1988). Synaptic activation of *N*-methyl-D-aspartate receptors in the Schaffer collateral–commissural pathway of rat hippocampus. *Journal of Physiology* **399**, 283–300.

COLLINGRIDGE, G. L. & SINGER, W. (1990). Excitatory amino acid receptors and synaptic plasticity. *Trends in Pharmacological Sciences* **11**, 290–296.

COLQUHOUN, D. & HAWKES, A. G. (1981). On the stochastic properties of single ion channels. *Proceedings of the Royal Society* B **211**, 205–235.

COLQUHOUN, D. & HAWKES, A. G. (1982). On the stochastic properties of bursts of single ion channel openings, and of clusters of bursts. *Philosophical Transactions of the Royal Society* B **300**, 1–59.

COLQUHOUN, D. & HAWKES, A. G. (1987). A note on correlations in single ion channel records. *Proceedings of the Royal Society* B **230**, 15–52.

COLQUHOUN, D., JONAS, P. & SAKMANN, B. (1992). Onset and offset of glutamate action on non-NMDA receptors, measured by concentration-jumps on patches from hippocampal neurones in rat brain slices. *Journal of Physiology* (in the Press).

COLQUHOUN, D. & SAKMANN, B. (1981). Fluctuations in the microsecond time range of the current through single acetylcholine-receptor ion channels. *Nature* **294**, 464–466.

COLQUHOUN, D. & SAKMANN, B. (1985). Fast events in single-channel currents activated by acetylcholine and its analogues in the frog muscle end-plate. *Journal of Physiology* **369**, 501–557.

COLQUHOUN, D. & SIGWORTH, F. J. (1983). Fitting and statistical analysis of single-channel records. In *Single-Channel Recording*, ed. SAKMANN, B. & NEHER, E., pp. 191–263. Plenum Press, New York, London.

COVARRUBIAS, M. & STEINBACH, J. H. (1990). Excision of membrane patches reduced the mean open time of nicotinic acetylcholine receptors. *Pflügers Archiv* **416**, 385–392.

CULL-CANDY, S. G. & PARKER, I. (1982). Rapid kinetics of single glutamate-receptor channels. *Nature* **295**, 410–412.

CULL-CANDY, S. G. & USOWICZ, M. M. (1987). Multiple-conductance channels activated by excitatory amino acids in cerebellar neurons. *Nature* **352**, 525–528.

CULL-CANDY, S. G. & USOWICZ, M. M. (1989). On the multiple-conductance single channels activated by excitatory amino acids in large cerebellar neurones of the rat. *Journal of Physiology* **415**, 555–582.

DALE, N. & ROBERTS, A. (1985). Dual-component amino-acid-mediated synaptic potentials: excitatory drive for swimming in *Xenopus* embryos. *Journal of Physiology* **363**, 35–59.

EDWARDS, F. A., KONNERTH, A., SAKMANN, B. & TAKAHASHI, T. (1989). A thin slice preparation for patch clamp recordings from synaptically connected neurones of the mammalian central nervous system. *Pflügers Archiv* **414**, 600–612.

FREDKIN, D. R., MONTAL, M. & RICE, J. A. (1985). Identification of aggregated Markovian models: application to the nicotinic acetylcholine receptor. From *Proceedings of the Berkeley Conference in Honor of Jerzy Neuman and Jack Kiefer*, ed. LE CAM, L. M. & OLSHEN, R. A., vol. 1, pp. 269–289. Wadsworth, Monterey, CA, USA.

FORSYTHE, I. D. & WESTBROOK, G. L. (1988). Slow excitatory postsynaptic currents mediated by *N*-methyl-D-aspartate receptors on cultured mouse central neurones. *Journal of Physiology* **396**, 515–533.

GIBB, A. J. (1989). Characteristics of channel openings activated by low concentrations of glutamate in cells dissociated from adult rat hippocampus. *Journal of Physiology* **415**, 39*P*.

GIBB, A. J. (1990). Clusters of NMDA receptor-channel openings are activated by low concentrations of L-glutamate in dissociated hippocampal cells of adult rat. *Journal of Physiology* **426**, 52*P*.

GIBB, A. J. & COLQUHOUN, D. (1991). Glutamate activation of a single NMDA receptor-channel produces a cluster of channel openings. *Proceedings of the Royal Society* B **243**, 39–45.

GIBB, A. J. & EDWARDS, F. A. (1991). Glycine does not influence the properties of single clusters of NMDA channel openings in outside-out patches from rat hippocampal granule cells. *Journal of Physiology* **437**, 122*P*.

HAMILL, O. P., MARTY, A., NEHER, E., SAKMANN, B. & SIGWORTH, F. J. (1981). Improved patch-clamp techniques for high-resolution current recording from cells and cell-free membrane patches. *Pflügers Archiv* **391**, 85–100.

HAWKES, A. G., JALALI, A. & COLQUHOUN, D. (1992). Asymptotic distributions of apparent open

times and shut times in a single channel record allowing for the omission of brief events. *Philosophical Transactions of the Royal Society* B **337**, 383–404.

HERRON, C. E., LESTER, R. A. J., COAN, E. J. & COLLINGRIDGE, G. L. (1986). Frequency-dependent involvement of NMDA receptors in the hippocampus: a novel synaptic mechanism. *Nature* **322**, 265–268.

HESTRIN, S., NICOLL, R. A., PERKEL, D. J. & SAH, P. (1990*a*). Analysis of excitatory synaptic action in pyramidal cells using whole-cell recording from rat hippocampal slices. *Journal of Physiology* **422**, 203–225.

HESTRIN, S., SAH, P. & NICOLL, R. A. (1990*b*). Mechanisms generating the time course of dual component excitatory synaptic currents recorded in hippocampal slices. *Neuron* **5**, 247–253.

HOWE, J. R., COLQUHOUN, D. & CULL-CANDY, S. G. (1988). On the kinetics of large-conductance glutamate-receptor ion channels in rat cerebellar granule neurons. *Proceedings of the Royal Society* B **233**, 407–422.

HOWE, J. R., CULL-CANDY, S. G. & COLQUHOUN, D. (1991). Currents through single glutamate-receptor channels in outside-out patches from rat cerebellar granule cells. *Journal of Physiology* **432**, 143–202.

JAHR, C. E. & STEVENS, C. F. (1987). Glutamate activates multiple single channel conductances in hippocampal neurons. *Nature* **325**, 522–525.

JAHR, C. E. & STEVENS, C. F. (1990). A quantitative description of NMDA receptor-channel kinetic behaviour. *Journal of Neuroscience* **10**, 1830–1837.

JOHNSON, J. W. & ASCHER, P. (1987). Glycine potentiates the NMDA response of mouse central neurones. *Nature* **325**, 529–531.

KAY, A. R. & WONG, R. K. S. (1986). Isolation of neurones suitable for patch-clamping from adult mammalian central nervous systems. *Journal of Neuroscience Methods* **16**, 227–238.

KELLER, B. U., KONNERTH, A. & YARRI, Y. (1991). Patch clamp analysis of excitatory synaptic currents in granule cells of rat hippocampus. *Journal of Physiology* **435**, 275–294.

KISKIN, N. I., KRISHTAL, O. A. & TSYNDRENKO, A. YA. (1990). Cross-desensitization reveals pharmacological specificity of excitatory amino acid receptors in isolated hippocampal neurons. *European Journal of Neuroscience* **2**, 461–470.

LÄUGER, P. (1983). Conformational transitions in ionic channels. In *Single-Channel Recording*, ed. SAKMANN, B. & NEHER, E., pp. 177–190. Plenum Press, New York, London.

LERMA, J., ZUKIN, R. S. & BENNETT, M. V. L. (1990). Glycine decreases desensitization of *N*-methyl-D-aspartate (NMDA) receptors expressed in *Xenopus* oocytes and is required for NMDA responses. *Proceedings of the National Academy of Sciences of the USA* **87**, 2354–2358.

LESTER, R. A. J., CLEMENTS, J. D., WESTBROOK, G. L. & JAHR, C. E. (1990). Channel kinetics determine the time course of NMDA-receptor mediated synaptic currents. *Nature* **346**, 565–567.

MCMANUS, O. B., BLATZ, A. L. & MAGLEBY, K. L. (1985). Inverse relationship of the durations of adjacent open and shut intervals for Cl and K channels. *Nature* **317**, 625–627.

MCMANUS, O. B. & MAGLEBY, K. L. (1989). Kinetic time constants independent of previous single-channel activity suggest Markov gating for a large conductance Ca-activated K channel. *Journal of General Physiology* **94**, 1037–1070.

MATHIE, A., COLQUHOUN, D. & CULL-CANDY, S. G. (1991). Conductance and kinetic properties of single channel currents through nicotinic acetylcholine receptor channels in rat sympathetic ganglion neurones. *Journal of Physiology* **439**, 717–750.

MATHIE, A., CULL-CANDY, S. G. & COLQUHOUN, D. (1987). Single channel and whole-cell currents evoked by acetylcholine in dissociated sympathetic neurones of the rat. *Proceedings of the Royal Society* B **232**, 239–248.

MAYER, M. L., VYKLICKY, L. & CLEMENTS, J. (1989). Regulation of NMDA receptor desensitization in mouse hippocampal neurons by glycine. *Nature* **338**, 425–427.

MITTMAN, S., TAYLOR, W. R. & COPENHAGEN, D. R. (1990). Concomitant activation of two types of glutamate receptor mediates excitation of salamander retinal ganglion cells. *Journal of Physiology* **428**, 175–197.

NOWAK, L., BREGESTOVSKI, P., ASCHER, P., HERBET, A. & PROCHIANTZ, A. (1984). Magnesium gates glutamate-activated channels in mouse central neurones. *Nature* **307**, 462–465.

RANDALL, A. D. & COLLINGRIDGE, G. L. (1991). Kinetic properties of NMDA and AMPA receptor-mediated EPSCs recorded from rat hippocampal slices under whole-cell voltage clamp. *Journal of Physiology* **435**, 41*P*.

SATHER, W., JOHNSON, J. W., HENDERSON, G. & ASCHER, P. (1990). Glycine-insensitive desensitization of NMDA responses in cultured mouse embryonic neurons. *Neuron* **4**, 725–731.

SIGWORTH, F. J. & SINE, S. M. (1987). Data transformation for improved display and fitting of single channel dwell time histograms. *Biophysical Journal* **52**, 1047–1054.

SINE, S. M., CLAUDIO, T. & SIGWORTH, F. J. (1990). Activation of Torpedo acetylcholine receptors expressed in mouse fibroblasts: single channel current kinetics reveal distinct agonist binding affinities. *Journal of General Physiology* **96**, 395–437.

SINE, S. M. & STEINBACH, J. H. (1986). Activation of acetylcholine receptors on clonal mammalian BC3H-1 cells by low concentration of agonist. *Journal of Physiology* **373**, 129–162.

SINE, S. M. & STEINBACH, J. H. (1987). Activation of acetylcholine receptors on clonal mammalian BC3H-1 cells by high concentrations of agonist. *Journal of Physiology* **385**, 325–359.

STERN, P., EDWARDS, F. A. & SAKMANN, B. (1992). Fast and slow components of unitary EPSCs on stellate cells elicited by focal stimulation in slices of rat visual cortex. *Journal of Physiology* **449**, 247–278.

THOMSON, A. M., WALKER, V. E. & FLYNN, D. M. (1989). Glycine enhances NMDA-receptor mediated synaptic potentials in neocortical slices. *Natural* **338**, 422–424.

TRAUTMANN, A. & SIEGELBAUM, S. A. (1983). The influence of membrane patch isolation on single acetylcholine-channel current in rat myotubes. In *Single-Channel Recording*, ed. SAKMANN, B. & NEHER, E., pp. 191–263. Plenum Press, New York, London.

TRAYNELIS, S. F. & CULL-CANDY, S. G. (1991). Pharmacological properties and H^+ sensitivity of excitatory amino acid receptor channels in rat cerebellar granule neurones. *Journal of Physiology* **433**, 727–763.

TWYMAN, R. E. & MACDONALD, R. L. (1991). Kinetic properties of the glycine receptor main- and sub-conductance states of mouse spinal cord neurones in culture. *Journal of Physiology* **435**, 303–332.

TWYMAN, R. E., ROGERS, C. J. & MACDONALD, R. L. (1990). Intraburst kinetic properties of the $GABA_A$ receptor main conductance state of mouse spinal cord neurones in culture. *Journal of Physiology* **423**, 193–219.

WATHEY, J. C. (1990). Computer simulations of quantal events mediated by NMDA receptors. *Society for Neuroscience Abstracts* **16**, 39.7.

WEISS, D. S. & MAGLEBY, K. L. (1989). Gating scheme for single GABA-activated Cl^- channels determined from stability plots, dwell-time distributions, and adjacent interval durations. *Journal of Neuroscience* **9**, 1316–1324.